Computers, Materials & Continua

Tech Science Press

https://doi.org/10.32604/cmc.2026.084242

ARTICLE

Enhanced Artificial Protozoa Optimizer via a Multi-Strategy Framework for Engineering Design Problems

Dingfeng Song[1], Haibo Wang[2,3,*], Zhiwei Ye[1], Shuhao Yang[1] and Mengxuan Li[1]

[1]School of Computer Science and Artificial Intelligence, Hubei University of Technology, Wuhan, China
[2]School of Economics and Management, Hubei University of Technology, Wuhan, China
[3]Digital Economy Development Research Center, Hubei University of Technology, Wuhan, China

*Corresponding Author: Haibo Wang. Email: 20051048@hbut.edu.cn

Received: 18 April 2026; Accepted: 03 August 2026; Published: 15 September 2026

ABSTRACT: The Artificial Protozoa Optimizer (APO) is a population-based metaheuristic for numerical optimization and engineering design. However, its stochastic initialization and limited local refinement can reduce performance on non-convex, discontinuous, and high-dimensional landscapes. To address these issues, this paper proposes an enhanced Artificial Protozoa Optimizer with a multi-strategy framework (EAPO). The method incorporates three mechanisms: a Symmetry-Enhanced Latin Hypercube Initialization (SELHI) strategy to improve the uniformity of the initial population, an Adaptive Phase Equilibrium Strategy (APES) to regulate the exploration–exploitation balance using iteration progress and population diversity, and an Adaptive Elite Perturbation Strategy (AEPS) to strengthen local refinement around high-quality individuals. Experiments on the CEC2005 and CEC2017 benchmark suites and five constrained engineering design problems show that EAPO improves upon the baseline APO and remains competitive with the selected comparison algorithms in solution quality, convergence behavior, and stability. Two-sided Wilcoxon rank-sum tests with Holm–Bonferroni correction indicate that many of these improvements are statistically significant. These results suggest that combining more uniform initialization, diversity-aware phase regulation, and elite-guided perturbation can improve APO on complex continuous and engineering optimization tasks.

KEYWORDS: Artificial Protozoa Optimizer; metaheuristic optimization; population-based search; exploration–exploitation balance; engineering design

1 Introduction

Optimization problems are ubiquitous in scientific and engineering domains, ranging from mechanical design and production scheduling to automatic control, signal processing, and computer vision [1]. With rapid technological development, these problems have grown increasingly complex, often involving non-convex, discontinuous, constrained, and high-dimensional search spaces [2,3]. Such landscapes frequently contain numerous local optima and ill-conditioned regions, making premature convergence a persistent challenge in complex engineering design. Traditional mathematical optimization techniques, which usually rely on assumptions such as convexity or differentiability, are ill-suited to these settings and often fail in the presence of multimodality or noise. The No Free Lunch theorem also suggests that no single optimizer can remain dominant across all problem classes [4]; therefore, improving a recent optimizer for specific difficult landscapes remains meaningful when the modification is supported by mechanism-level analysis and fair empirical comparison.

These limitations have fueled the development of metaheuristic algorithms, which are nature-inspired computational methods capable of solving complex optimization problems without requiring strong structural assumptions [5,6]. Swarm intelligence techniques, in particular, have achieved remarkable success by simulating the collective behavior of biological and physical systems, such as flocking birds, schooling fish, or hunting wolves [7]. Representative examples include Particle Swarm Optimization (PSO) [8], Grey Wolf Optimizer (GWO) [9], and Whale Optimization Algorithm (WOA) [10]. Recent studies continue to propose new and hybrid metaheuristics for engineering and numerical optimization, including red-crowned crane optimization and ensemble population-based designs [11,12]. Human-inspired search strategies have also been explored [13], while a modified APO variant has recently been applied to nonlinear system identification [14]. Despite their success, these approaches still face challenges such as premature convergence, stagnation, and parameter sensitivity, especially in high-dimensional and multimodal problems [15].

The Artificial Protozoa Optimizer (APO) [16] is a recently proposed metaheuristic that balances exploration and exploitation through population-level update operators. Although APO has demonstrated competitive results, it still suffers from several structural drawbacks [17]: (i) reliance on random initialization, which may create clustered samples and leave parts of the search space insufficiently explored; (ii) limited feedback from population diversity when switching between search phases, which can weaken the response to diversity collapse; and (iii) insufficient use of elite statistical information for late-stage local refinement. These factors can make APO prone to premature convergence in non-convex, high-dimensional, and constrained engineering problems.

To address these shortcomings, this paper proposes an Enhanced Artificial Protozoa Optimizer with a multi-strategy framework (EAPO), an improved APO variant. The novelty of EAPO lies in assigning complementary roles to three mechanisms at different stages of the search rather than merely adding extra random perturbations. The main innovations of EAPO are as follows:

- A **Symmetry-Enhanced Latin Hypercube Initialization (SELHI)** mechanism that uses orthogonal-rotation symmetry to remove sampling bias, thereby improving population diversity and ensuring uniform coverage of the search space.
- An **Adaptive Phase Equilibrium Strategy (APES)** that provides a population-diversity feedback framework to dynamically regulate the exploration–exploitation balance across search phases.
- An **Adaptive Elite Perturbation Strategy (AEPS)** that uses elite statistics (mean and standard deviation) to guide efficient local refinement of top individuals and reduce stagnation.

The paper is structured as follows. Section 2 reviews the baseline APO framework. Section 3 presents the three EAPO enhancements. Section 4 reports the experimental setup and results. Section 5 concludes and outlines future work.

2 Overview of Artificial Protozoa Optimizer

APO is a population-based metaheuristic motivated by adaptive protozoan behavior in changing environments [16,17]. In the original algorithm, each iteration mainly consists of two foraging updates: autotrophic foraging, which favors exploration of the search space, and heterotrophic foraging, which emphasizes search around better solutions. In addition, dormancy and reproduction are triggered with certain probabilities to reintroduce diversity and preserve advantageous individuals. These four operators together define the basic search process of APO.

2.1 Population Initialization

APO uses stochastic uniform initialization within the search bounds. For the j-th dimension of the i-th individual:

$$x_i^j = lb_j + r_{ij} \cdot (ub_j - lb_j), \quad r_{ij} \sim \mathcal{U}(0,1), \tag{1}$$

where lb_j and ub_j are the lower and upper bounds of the j-th variable, respectively. The original APO adopts this scheme mainly because it is simple, parameter-free, and computationally inexpensive. However, purely random samples may be unevenly distributed when the dimension is high or the feasible region is narrow, which motivates the SELHI mechanism introduced in Section 3.

2.2 Core Update Rules

APO uses different operators for foraging, dormancy (encystment), and reproduction. In this study, the original APO operators are retained, while the three proposed modules are inserted around them. Specifically, autotrophic foraging is used as the main exploratory mode, heterotrophic foraging promotes movement around more promising regions, dormancy regenerates weak individuals to restore diversity, and reproduction preserves and recombines advantageous individuals. The implementation follows the original APO formulation [16]; EAPO modifies only the initialization, phase-selection control, and elite-refinement stages described in Section 3. This separation helps distinguish the baseline APO behavior from the proposed enhancements.

3 Enhanced Artificial Protozoa Optimizer with Multi-Strategies

The baseline APO achieves a balance between exploration and exploitation through mechanisms such as autotrophic/heterotrophic foraging, encystment, and reproduction. Nevertheless, two major limitations persist: (i) insufficient initial population diversity, which may undermine global search efficiency, and (ii) susceptibility to stagnation in highly multimodal landscapes [2,3]. To address these challenges, we propose *EAPO*, which incorporates three complementary enhancements designed to strengthen early exploration, regulate search dynamics throughout iterations, and provide progressively finer elite refinement in later iterations. The design of these mechanisms follows population-level principles of diversity preservation, adaptive phase regulation, and elite-guided refinement. The overall framework of EAPO is illustrated in Fig. 1.

3.1 Symmetry-Enhanced Latin Hypercube Initialization (SELHI)

The first innovation of EAPO is a refined initialization strategy, termed SELHI. Biologically, protozoa in heterogeneous environments tend to disperse to reduce intra-species competition, and their trajectories often exhibit symmetric spread around local stimuli, which helps cover multiple micro-niches. SELHI translates this behavior into a space-filling initialization by integrating Latin Hypercube Sampling (LHS) with orthogonal-rotation symmetry and distance-based dispersion refinement. The synergy of these components systematically reduces sampling bias, improves global coverage, and significantly increases the probability of locating promising regions at the outset of the optimization process.

Unlike conventional uniform random initialization, LHS divides each dimension into equiprobable intervals, ensuring that one candidate solution is sampled per interval. This guarantees more uniform coverage of the search space, particularly in high-dimensional or multimodal problems. Related evidence also indicates that quasi-random or low-discrepancy sampling can improve population-based optimization performance by reducing initialization bias [18,19], while opposition-based initialization can enlarge the sampled region by generating paired candidates [20]. SELHI follows this general motivation of improving initial coverage, but further applies an orthogonal rotation in normalized space to create a symmetric counterpart for each candidate and then performs a local dispersion refinement that repels points from their neighborhood centers. This dual mechanism mitigates the risk of clustered samples and provides a stronger foundation for subsequent optimization.

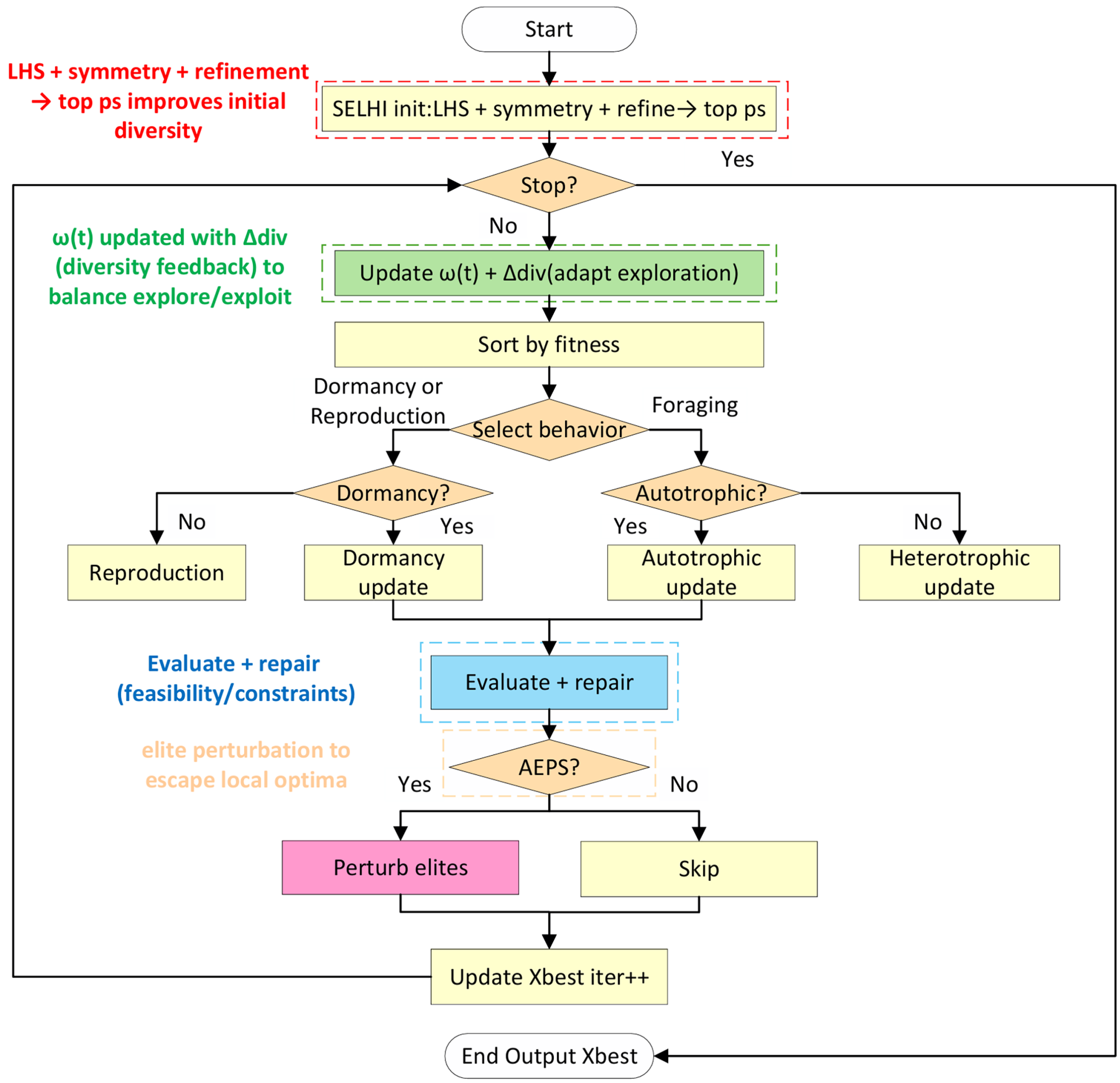

Figure 1: Framework of EAPO.

Empirical evidence suggests that uniform random sampling often results in clustered and uneven distributions, leaving large portions of the search space unexplored. In contrast, the LHS with orthogonal-rotation symmetry and dispersion refinement employed in SELHI yields broader coverage and better dispersion, thereby enhancing both efficiency and robustness in the early stage of optimization. Fig. 2 visualizes the coverage advantage of SELHI over conventional random initialization.

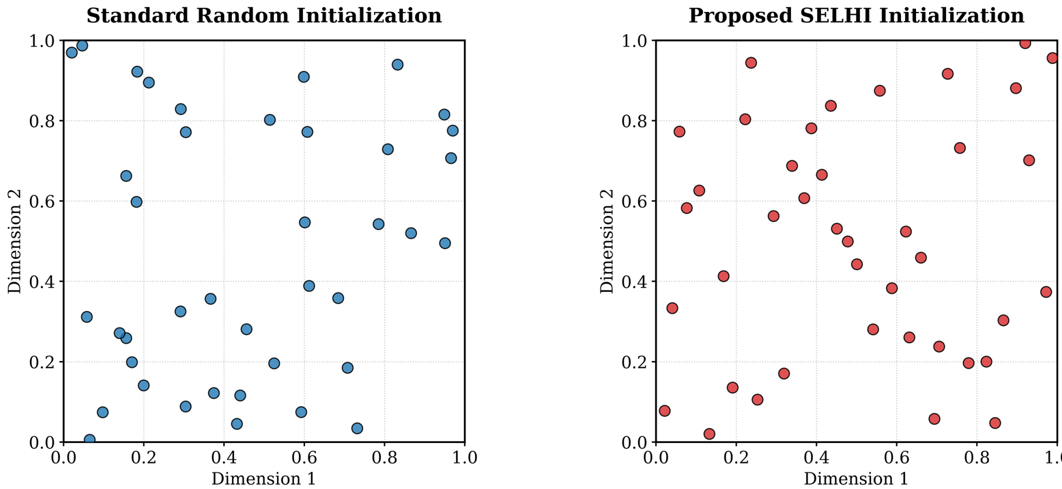

Figure 2: SELHI initialization comparison: coverage differences between conventional random sampling and the proposed SELHI mechanism.

Formally, the LHS-based initialization in dimension j partitions the interval $[lb_j, ub_j]$ into ps subintervals. With a randomly permuted sequence π_j and a uniform random variable u_{ij}, the i-th sampling point is given by:

$$x_i^j = lb_j + \left(\frac{\pi_j(i) - 1 + u_{ij}}{ps}\right)(ub_j - lb_j), \quad i = 1, \ldots, ps, \; j = 1, \ldots, \dim. \tag{2}$$

Subsequently, an orthogonal-rotation symmetry is applied in the normalized space to generate a rotated counterpart:

$$x_i^{\text{rot}} = lb + (0.5 + (u_i - 0.5)R) \odot (ub - lb), \quad u_i = \frac{x_i - lb}{ub - lb}, \tag{3}$$

where R is an orthogonal matrix (generated by QR decomposition of a random Gaussian matrix) and $\odot$ denotes elementwise multiplication. A distance-based dispersion refinement is then applied:

$$x_i^{\text{ref}} = x_i^{\text{rot}} + \rho \cdot \frac{x_i^{\text{rot}} - \bar{x}_{N_k(i)}}{\left\| x_i^{\text{rot}} - \bar{x}_{N_k(i)} \right\| + \varepsilon}, \tag{4}$$

where $\bar{x}_{N_k(i)}$ is the mean of the k nearest neighbors of x_i^{rot}, ρ is a small dispersion coefficient, and ε avoids division by zero. The combined population X_{combined} of size $2ps$ (from X and X^{ref}) is then evaluated, and the top ps individuals are retained according to their fitness ranking, as defined in Eq. (5):

$$\text{rank}(X_i) = \sum_{X_m \neq X_i} \mathbf{1}\left[\varphi(X_m) < \varphi(X_i)\right], \tag{5}$$

where $\text{rank}(X_i)$ denotes the rank of candidate X_i, and $\varphi(\cdot)$ is the fitness value to be minimized.

3.2 Adaptive Phase Equilibrium Strategy (APES)

The second innovation, termed Adaptive Phase Equilibrium Strategy (APES), introduces a dynamic control law that balances global exploration and local exploitation during the optimization process. Instead of fixed parameters, APES adjusts search intensity using both iteration progress and a diversity feedback signal.

Formally, the exploration-to-exploitation ratio is modeled as a monotonically decreasing function of the iteration index t:

$$\omega(t) = \omega_{\max} - (\omega_{\max} - \omega_{\min}) \cdot \left(\frac{t}{T_{\max}}\right)^{\kappa}, \tag{6}$$

where $\omega(t)$ denotes the exploration weight at iteration t, $\omega_{\max}$ and $\omega_{\min}$ represent the initial and final bounds, $T_{\max}$ is the maximum number of iterations (set to $\text{iter}_{\max}$ in Algorithm 1), and κ controls the decay rate. A larger κ favors sustained exploration in the early phase, while a smaller κ accelerates the transition toward exploitation. In practice, $\omega_{\max}$ and $\omega_{\min}$ are set within $(0, 1)$ so that $\omega(t)$ can be interpreted as the probability of selecting the exploration (autotrophic) mode.

APES further introduces a diversity feedback mechanism by monitoring the average pairwise distance Δ_{div} within the population. When Δ_{div} falls below a threshold $\Delta_{\min}$, the exploration weight is temporarily increased:

$$\widetilde{\omega}(t) = \min(\omega_{\max},\ \omega(t) + \zeta \cdot \max(0, \Delta_{\min} - \Delta_{\text{div}})), \tag{7}$$

where $\zeta > 0$ controls the feedback strength; otherwise, $\widetilde{\omega}(t) = \omega(t)$. In EAPO, $\widetilde{\omega}(t)$ directly controls foraging-mode selection: higher values increase the probability of using the autotrophic (exploration) update, while lower values favor the heterotrophic (exploitation) update. This makes $\omega(t)$ evolve dynamically with both iteration count and population state, reducing premature convergence on complex multimodal landscapes. The diversity metric is defined as the normalized average pairwise distance:

$$\Delta_{\text{div}} = \frac{2}{ps(ps-1)} \sum_{i<j} \frac{\|X_i - X_j\|_2}{\|ub - lb\|_2}, \tag{8}$$

where normalization by $\|ub - lb\|_2$ keeps $\Delta_{\text{div}} \in (0, 1)$ for bounded search spaces. Fig. 3 shows the diversity dynamics with APES, highlighting how the feedback mechanism increases exploration when Δ_{div} approaches the $\Delta_{\min}$ threshold.

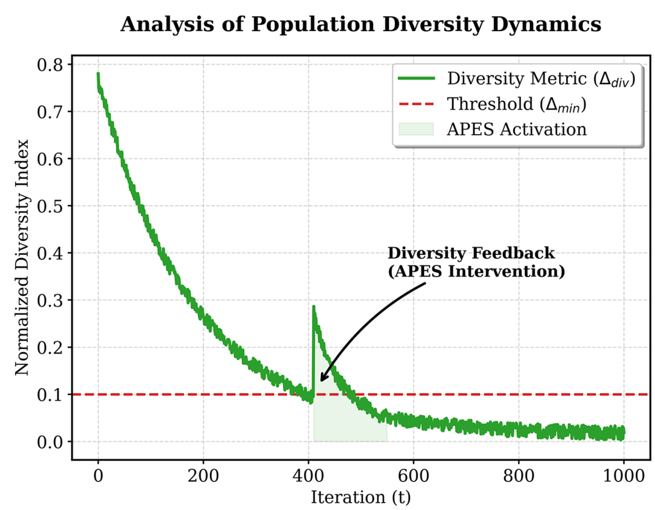

Figure 3: Population diversity dynamics under APES: feedback around $\Delta_{\min}$ triggers increased exploration to counter diversity collapse.

3.3 *Adaptive Elite Perturbation Strategy (AEPS)*

The third innovation, termed *Adaptive Elite Perturbation Strategy (AEPS)*, refines the exploitation ability of EAPO through statistics-guided local perturbations of top-performing individuals. AEPS operates after the canonical foraging, dormancy, and reproduction stages to intensify local search while preserving sufficient variability to escape local optima.

3.3.1 Mechanism Overview

AEPS selects the top p_e fraction of the population as the elite subset based on fitness. To prevent premature convergence, an elite-statistics-guided perturbation generates new candidate solutions around elite individuals. The perturbation is expressed as:

$$\widetilde{X}_i = X_{e_1} + \eta(t) \odot (\mu_e - X_{e_1}) + \sigma_e \odot \mathcal{N}(\mathbf{0}, I) \tag{9}$$

where $\widetilde{X}_i$ is the perturbed candidate, X_{e_1} is a selected elite parent, μ_e and σ_e are the mean and per-dimension standard deviation of the elite set, and $\eta(t)$ is a time-varying attraction weight that decreases with iterations:

$$\eta(t) = \eta_{\max} - (\eta_{\max} - \eta_{\min}) \cdot \frac{t}{T_{\max}}, \quad \eta_{\max} > \eta_{\min} > 0. \tag{10}$$

Early in the search, larger $\eta(t)$ pulls elites toward the elite mean to accelerate coarse convergence; later, smaller $\eta(t)$ yields finer perturbations for local refinement. To maintain feasibility, the boundary condition is enforced as:

$$\widetilde{x}_i^j = \max\left(lb_j, \min(\widetilde{x}_i^j, ub_j)\right) \tag{11}$$

If $\widetilde{X}_i$ exhibits superior fitness, it replaces its parent in the elite pool. Formally, the population update is given by Eq. (12):

$$X_{pop}^{(t+1)} = \mathrm{TopFitness}\left(X_{pop}^{(t)} \cup \{\widetilde{X}_1, \ldots, \widetilde{X}_{N_{\mathrm{elite}}}\}, ps\right) \tag{12}$$

where $N_{\mathrm{elite}} = p_e \cdot ps$, and $\mathrm{TopFitness}(\cdot)$ selects the best ps candidates by fitness. This adaptive perturbation enables EAPO to exploit promising regions more effectively, while ensuring sufficient variability to escape local optima.

3.4 *EAPO Algorithm Outline*

Algorithm 1 summarizes the proposed EAPO. Built on the baseline APO, EAPO introduces three modules: SELHI improves the initial population by combining LHS, rotational symmetry, and dispersion refinement; APES regulates the exploration–exploitation balance through the scheduled weight $\omega(t)$ and the diversity-corrected weight $\widetilde{\omega}(t)$; and AEPS perturbs elite individuals according to elite statistics, with $\eta(t)$ gradually decreasing from coarse guidance to fine local refinement. Together with the original foraging, dormancy, and reproduction operators, these modules define the complete search procedure.

Algorithm 1: Enhanced artificial protozoa optimizer with multi-strategies (EAPO)

Require: Population size ps, dimension dim, max iterations $\mathrm{iter}_{\max}$, bounds $\{lb_j, ub_j\}$, and control parameters $\Theta = \{\omega_{\max}, \omega_{\min}, \kappa, \Delta_{\min}, p_e, \eta_{\min}, \eta_{\max}, p_d, p_r, \rho, k, \varepsilon\}$
Ensure: Best solution X_{best}

(Continued)

Algorithm 1 (continued)

1. Initialization (SELHI)

Generate ps LHS samples; construct rotated and refined candidates using Eqs. (2)–(4)
Merge all candidates, retain the top ps, and initialize X_{best}
iter $\leftarrow 0$

2. Main Evolutionary Loop

while iter $<$ iter$_{\max}$ **do**
  Update $\omega(t)$ and $\widetilde{\omega}(t)$ using Eqs. (6) and (7); sort the population by fitness
  for $i = 1$ to ps **do**
    Generate candidate $\widehat{X}_i$ by autotrophic or heterotrophic foraging according to $\widetilde{\omega}(t)$
    Apply dormancy with probability p_d; otherwise apply reproduction with probability p_r
    Repair bounds/discrete variables, evaluate $\widehat{X}_i$, and keep the better of $\{X_i, \widehat{X}_i\}$ using the feasibility rules in Section 4.5.1
  end for

3. Elite Perturbation (AEPS)

  Form an elite set of size $N_{\text{elite}} = \lfloor p_e \cdot ps \rfloor$, update $\eta(t)$ (Eq. (10)), and compute μ_e, σ_e
  for each elite parent X_{e_1} **do**
    Generate $\widetilde{X} = X_{e_1} + \eta(t) \odot (\mu_e - X_{e_1}) + \sigma_e \odot \mathcal{N}(\mathbf{0}, I)$ (Eq. (9))
    Repair, evaluate, and replace X_{e_1} if $\widetilde{X}$ is better under the feasibility rules
  end for
  Update X_{best} if improved; iter $\leftarrow$ iter + 1
end while
return X_{best}

3.5 *Algorithm Complexity Analysis of EAPO*

Let ps be population size, dim dimension, iter$_{\max}$ iterations, and C_f fitness cost. Per iteration, APO operators and AEPS are $O(ps \cdot dim)$, sorting is $O(ps \log ps)$, and exact diversity computation using Eq. (8) is $O(ps^2 \cdot dim)$ because it requires all pairwise distances. Thus,

$$O\Big(\text{iter}_{\max} \times \big[ps^2 \cdot dim + ps\log(ps) + ps \cdot dim + ps \cdot C_f\big]\Big). \tag{13}$$

If only a diversity indicator is required for feedback, the pairwise term can be approximated by a centroid-based measure (mean and average distance to the centroid), by per-dimension variance, or by subsampling a small number of pairs. In these cases the diversity cost reduces to $O(ps \cdot dim)$ (or $O(m \cdot dim)$ for $m \ll ps^2$ sampled pairs), yielding

$$O\Big(\text{iter}_{\max} \times \big[ps\log(ps) + ps \cdot dim + ps \cdot C_f\big]\Big). \tag{14}$$

In practice, C_f dominates.

4 Experimental Results and Discussion

To ensure a fair comparison, the experimental environment is as follows: the operating system is Ubuntu 22.04, the CPU is Intel(R) Core(TM) i7-12700 2.10 GHz, the RAM is 64 GB, and the programming language is Python.

4.1 Experimental Protocol and Parameter Settings

The algorithms were tested on the standard CEC 2005 benchmark suite (CEC2005) following the official definitions. The experimental protocol, comparison algorithms, statistical settings, and EAPO control parameters are summarized in Table 1. For EAPO, the additional SELHI and AEPS candidate evaluations are counted within the same NFE budget, and the number of main-loop iterations is reduced accordingly. Detailed results for all 23 functions are reported in Table 2.

Table 1: Experimental protocol for the CEC2005 experiments.

Item	Setting
Benchmark suite	CEC2005 official definitions
Dimension	$D = 30$
Population size	$ps = 50$
Maximum evaluations	$B = 50{,}000$ NFE ($\approx 1667D$)
Independent runs	30
Randomness control	Recorded seeds; common noise stream for F4 and F17 within each run
Reported metric	Bias-corrected error, $f(x)$ − bias
Comparison algorithms	APO [16], CFOA [21], DE [15], GWO, HRO [22], PSA [23], SHIO [24], SSA [25], WOA
Baseline parameters	Recommended settings in the corresponding source papers
EAPO parameters	$\omega_{\max} = 0.9$, $\omega_{\min} = 0.1$, $\kappa = 2$, $\Delta_{\min} = 0.10$, $p_e = 0.20$, $\eta_{\max} = 0.5$, $\eta_{\min} = 0.1$, $\rho = 0.10$, $k = 3$, $\varepsilon = 1 \times 10^{-12}$, $p_d = p_r = 0.1$
Statistical test	Two-sided Wilcoxon rank-sum test with Holm–Bonferroni correction, $\alpha = 0.05$

4.2 CEC2005 Benchmark Experiments

The CEC2005 suite (23 shifted/rotated functions, dimension $D = 30$) is used as the primary continuous benchmark. Results are reported as bias-corrected errors ($f(x)$ − bias), so the optimum is 0 for all functions.

4.2.1 Result Statistics and Convergence Curve Analysis

Based on the comprehensive results in Table 2, EAPO is among the top performers across the benchmark functions. Among the 23 test functions, EAPO attains the best average value on 20 functions (86.96%) and the best optimal value on 19 functions (82.61%). It also exhibits the lowest standard deviation on 16 functions (69.57%) and the best median value on 20 functions (86.96%). Other algorithms achieve the best results on a few functions (e.g., GWO on F5 and F11, SSA on F8), indicating complementary strengths. Overall, EAPO maintains strong accuracy and stability on both unimodal and multimodal scenarios.

Table 2: Comparison results between EAPO and other algorithms on 23 benchmark functions. Best values are in bold.

Function	Metric	APO	CFOA	DE	GWO	HRO	EAPO	PSA	SHIO	SSA	WOA
F1	AVE	1.180180e−05	5.187107e+04	6.476741e+03	4.072787e+02	4.688938e+04	**1.619335e−07**	4.317540e+03	1.243629e+04	2.803813e−01	3.642045e+03
	Best	2.478218e−06	4.218011e+04	3.502345e+03	2.930284e+01	2.909642e+04	**9.518203e−09**	1.804757e+03	7.980454e+02	6.455620e−02	1.238341e+02
	Median	7.124579e−06	5.264709e+04	6.150108e+03	3.541832e+02	4.674748e+04	**9.758119e−08**	3.214219e+03	1.377411e+04	2.247536e−01	3.163135e+03
	Std	1.270438e−05	4.633923e+03	1.859431e+03	3.501153e+02	9.966450e+03	**1.806338e−07**	2.761043e+03	6.053762e+03	2.078758e−01	2.665832e+03
F2	AVE	2.314921e+03	7.685299e+04	2.940216e+04	5.974350e+03	5.035161e+04	**4.424660e+02**	3.930525e+04	1.996909e+04	2.681292e+04	5.043884e+04
	Best	1.235311e+03	5.126314e+04	1.231140e+04	2.077821e+03	3.259987e+04	**1.607962e+02**	2.722140e+04	1.136318e+04	1.850866e+04	3.203714e+04
	Median	2.103337e+03	7.175780e+04	2.886629e+04	5.796200e+03	4.788591e+04	**4.451361e+02**	3.548206e+04	1.982525e+04	2.551721e+04	4.952967e+04
	Std	9.178159e+02	2.011930e+04	6.669261e+03	2.608605e+03	1.273102e+04	**1.499629e+02**	1.132821e+04	4.869274e+03	5.648638e+03	9.094657e+03
F3	AVE	2.280835e+07	1.573629e+12	5.557163e+10	1.336654e+09	1.464387e+12	**3.067573e+06**	4.757061e+10	2.601154e+10	1.271837e+10	1.303564e+10
	Best	7.257300e+06	8.351989e+11	1.799591e+10	1.314355e+08	3.521942e+11	**4.134421e+05**	1.440766e+10	2.249601e+09	1.527326e+07	1.501904e+09
	Median	1.550885e+07	1.348421e+12	5.186222e+10	1.118651e+09	1.121759e+12	**2.865256e+06**	3.514684e+10	2.031726e+10	1.647078e+08	8.652845e+09
	Std	1.947024e+07	7.647497e+11	3.110277e+10	1.318245e+09	1.132521e+12	**1.945088e+06**	4.388290e+10	1.919074e+10	3.008199e+10	1.183372e+10
F4	AVE	9.140351e+03	8.176830e+04	4.366074e+04	1.033050e+04	4.160467e+04	**4.142684e+03**	5.684837e+04	2.152874e+04	5.183351e+04	1.496071e+05
	Best	5.914492e+03	5.633336e+04	2.789418e+04	4.015944e+03	2.836233e+04	**7.826588e+02**	4.083179e+04	1.077425e+04	3.331264e+04	8.390449e+04
	Median	8.465475e+03	8.109094e+04	4.411658e+04	1.032875e+04	4.040279e+04	**4.462985e+03**	5.466402e+04	2.053652e+04	5.309286e+04	1.434793e+05
	Std	2.782504e+03	1.922730e+04	7.690021e+03	2.935273e+03	9.132570e+03	**1.549199e+03**	1.176033e+04	6.518681e+03	1.006009e+04	4.831552e+04
F5	AVE	4.333253e+03	3.097152e+04	9.704023e+03	**3.045537e+03**	2.981527e+04	3.405112e+03	1.896696e+04	1.691909e+04	2.442453e+04	2.883950e+04
	Best	3.596191e+03	2.713793e+04	6.762570e+03	**5.663593e+02**	1.893326e+04	1.837616e+03	1.477369e+04	1.158410e+04	1.624276e+04	1.932129e+04
	Median	4.140771e+03	3.077569e+04	9.515547e+03	**1.783275e+03**	3.025578e+04	3.491496e+03	1.812260e+04	1.708516e+04	2.449176e+04	2.976396e+04
	Std	6.059659e+02	2.861417e+03	1.374023e+03	2.163031e+03	4.622899e+03	**4.681952e+02**	3.569122e+03	2.729769e+03	3.947747e+03	5.077149e+03
F6	AVE	6.685182e+02	2.183645e+10	4.226897e+08	1.035027e+07	1.709348e+10	**1.462125e+02**	4.078287e+08	3.790969e+09	3.159144e+03	1.474971e+08
	Best	1.175383e+02	1.409566e+10	1.823173e+08	7.781118e+03	1.072165e+10	**1.369123e+01**	2.970612e+07	1.771029e+07	2.931297e+02	7.987972e+05
	Median	2.076732e+02	2.002211e+10	4.019514e+08	2.360704e+06	1.617690e+10	**1.335471e+02**	6.251785e+07	3.612480e+09	1.442953e+03	1.634537e+07
	Std	1.807917e+03	7.162403e+09	1.731542e+08	1.590210e+07	4.460531e+09	**7.964233e+01**	1.088888e+09	2.526569e+09	4.337778e+03	3.921141e+08
F7	AVE	4.683869e+03	8.373369e+03	4.694862e+03	4.688103e+03	6.668057e+03	**4.683389e+03**	5.452835e+03	4.705839e+03	4.794197e+03	4.822950e+03
	Best	4.683214e+03	7.517181e+03	4.683103e+03	4.685871e+03	4.828343e+03	**4.683064e+03**	4.902584e+03	4.695890e+03	4.695572e+03	4.688156e+03
	Median	4.683240e+03	8.439515e+03	4.684141e+03	4.687598e+03	6.782790e+03	**4.683214e+03**	5.397178e+03	4.705001e+03	4.822472e+03	4.854413e+03
	Std	1.739277e+00	5.355720e+02	2.871442e+01	2.443519e+00	1.464421e+03	**4.029336e−01**	4.415174e+02	5.938542e+00	5.794537e+01	5.621321e+01
F8	AVE	2.105441e+01	2.119544e+01	2.103360e+01	2.101497e+01	2.108440e+01	2.101062e+01	2.104517e+01	2.103226e+01	**2.098607e+01**	2.102567e+01
	Best	2.099333e+01	2.113256e+01	2.090140e+01	2.085246e+01	2.095929e+01	2.093176e+01	2.099783e+01	2.090610e+01	**2.084909e+01**	2.092362e+01
	Median	2.104986e+01	2.119660e+01	2.104118e+01	2.103612e+01	2.109787e+01	2.101050e+01	2.104640e+01	2.103998e+01	**2.099003e+01**	2.103456e+01
	Std	2.963458e−02	4.007420e−02	5.069407e−02	5.910089e−02	5.417983e−02	3.613780e−02	**2.705621e−02**	5.421095e−02	5.281295e−02	5.523062e−02
F9	AVE	1.677384e+01	3.898434e+02	1.673255e+02	7.663516e+01	3.344066e+02	**1.289530e+01**	2.862078e+02	2.062443e+02	2.145568e+02	2.452381e+02
	Best	1.118828e+01	3.595515e+02	1.225352e+02	4.099809e+01	2.998413e+02	**8.155172e+00**	2.338386e+02	1.572951e+02	1.452346e+02	1.812812e+02
	Median	1.638948e+01	3.829303e+02	1.637360e+02	6.461151e+01	3.270947e+02	**1.316057e+01**	2.810161e+02	1.981379e+02	2.192878e+02	2.367096e+02
	Std	4.525685e+00	2.298636e+01	2.837176e+01	4.484759e+01	2.446134e+01	**2.420902e+00**	3.696190e+01	2.987243e+01	2.113031e+01	4.455249e+01

(Continued)

Table 2 (continued)

Function	Metric	APO	CFOA	DE	GWO	HRO	EAPO	PSA	SHIO	SSA	WOA
F10	AVE	4.759934e+01	6.127592e+02	3.217546e+02	1.437485e+02	5.500931e+02	**4.282746e+01**	4.248224e+02	3.327670e+02	4.714376e+02	4.897422e+02
	Best	3.734647e+01	5.401064e+02	2.712023e+02	5.316530e+01	4.314827e+02	**2.593930e+01**	3.708473e+02	2.263646e+02	3.288675e+02	3.252839e+02
	Median	4.629585e+01	6.128357e+02	3.221812e+02	1.419469e+02	5.421444e+02	**4.378200e+01**	4.195226e+02	3.293730e+02	4.491724e+02	4.913400e+02
	Std	7.644571e+00	4.029012e+01	2.036640e+01	7.046376e+01	5.512556e+01	**7.428818e+00**	4.642227e+01	5.530938e+01	9.439705e+01	7.938186e+01
F11	AVE	3.004370e+01	4.718447e+01	4.151551e+01	**1.779420e+01**	4.023984e+01	2.570904e+01	3.572617e+01	2.985888e+01	3.879723e+01	4.039863e+01
	Best	2.824384e+01	4.568331e+01	3.955156e+01	**1.127604e+01**	3.428292e+01	1.861842e+01	3.260303e+01	2.273845e+01	3.548985e+01	3.421006e+01
	Median	2.998081e+01	4.708345e+01	4.168084e+01	**1.807511e+01**	4.095474e+01	2.700154e+01	3.524889e+01	2.999875e+01	3.913598e+01	4.065894e+01
	Std	1.050306e+00	9.428029e−01	**9.104086e−01**	2.840538e+00	2.521763e+00	3.830663e+00	2.009109e+00	4.154357e+00	1.955767e+00	2.267894e+00
F12	AVE	2.831165e+04	1.193776e+06	4.578463e+05	6.040134e+04	1.027613e+06	**1.346712e+04**	2.406152e+05	2.240017e+05	5.743240e+04	2.074528e+05
	Best	1.586738e+04	9.461854e+05	2.324708e+05	1.321785e+04	6.004506e+05	**3.215828e+03**	1.682072e+05	6.204691e+04	1.973708e+04	1.855844e+04
	Median	2.411080e+04	1.113711e+06	4.310240e+05	5.781538e+04	1.013314e+06	**1.496152e+04**	2.278998e+05	2.253303e+05	5.567627e+04	1.684372e+05
	Std	1.089377e+04	2.060790e+05	1.448084e+05	2.722513e+04	2.389787e+05	**5.752327e+03**	6.684397e+04	9.584621e+04	2.297566e+04	1.361837e+05
F13	AVE	2.994036e+00	7.045537e+01	6.622135e+01	1.024965e+01	3.356887e+01	**2.389957e+00**	3.626853e+01	9.123774e+00	2.035680e+01	3.943332e+01
	Best	2.505679e+00	4.359729e+01	3.598553e+01	3.536514e+00	2.209721e+01	**1.797795e+00**	2.914672e+01	5.347276e+00	8.689894e+00	1.711669e+01
	Median	2.919758e+00	5.402481e+01	5.887728e+01	1.044241e+01	2.938028e+01	**2.426453e+00**	3.346309e+01	8.654167e+00	2.056960e+01	3.198897e+01
	Std	**3.418795e−01**	3.494354e+01	2.400349e+01	4.944445e+00	1.500454e+01	3.854120e−01	7.227230e+00	2.453696e+00	5.773201e+00	2.078442e+01
F14	AVE	1.270941e+01	1.432041e+01	1.384885e+01	1.255075e+01	1.334152e+01	**1.237908e+01**	1.349937e+01	1.275399e+01	1.334195e+01	1.358741e+01
	Best	1.245103e+01	1.419089e+01	1.354879e+01	**1.116142e+01**	1.253637e+01	1.201395e+01	1.322814e+01	1.211209e+01	1.260502e+01	1.297773e+01
	Median	1.267609e+01	1.431574e+01	1.384559e+01	1.251644e+01	1.335120e+01	**1.239445e+01**	1.346870e+01	1.269201e+01	1.336364e+01	1.358928e+01
	Std	1.571768e−01	**9.008638e−02**	1.029004e−01	5.452435e−01	3.924000e−01	2.304094e−01	1.713472e−01	3.573442e−01	2.899985e−01	3.004147e−01
F15	AVE	3.404292e+02	1.026232e+03	5.879613e+02	4.218172e+02	1.022013e+03	**2.421992e+02**	7.619296e+02	8.579894e+02	7.262488e+02	9.176796e+02
	Best	3.000190e+02	9.131775e+02	5.009741e+02	2.291751e+02	7.894514e+02	**2.000020e+02**	5.948903e+02	5.043749e+02	4.057091e+02	4.993527e+02
	Median	3.003327e+02	1.007416e+03	5.937819e+02	4.109355e+02	1.053607e+03	**2.007630e+02**	7.597489e+02	8.583341e+02	7.950644e+02	9.839817e+02
	Std	6.224470e+01	7.132272e+01	5.098330e+01	8.002670e+01	1.179508e+02	**4.814388e+01**	1.001950e+02	1.270865e+02	2.595268e+02	2.597110e+02
F16	AVE	1.426375e+02	7.880859e+02	3.615993e+02	3.114522e+02	7.803071e+02	**9.211801e+01**	5.029283e+02	5.845133e+02	5.855830e+02	6.594647e+02
	Best	5.860702e+01	6.454785e+02	3.164212e+02	9.773294e+01	5.278269e+02	**5.013125e+01**	4.229772e+02	2.916895e+02	3.871796e+02	4.805684e+02
	Median	7.586526e+01	7.708426e+02	3.478544e+02	2.503865e+02	7.860819e+02	**7.278975e+01**	4.869540e+02	6.213329e+02	5.899513e+02	6.360568e+02
	Std	1.312204e+02	1.019577e+02	**3.415980e+01**	1.743798e+02	1.375304e+02	4.082902e+01	7.173041e+01	1.370794e+02	9.543804e+01	1.122253e+02
F17	AVE	2.449347e+02	8.943616e+02	4.038667e+02	3.228877e+02	7.089364e+02	**8.398643e+01**	6.097410e+02	5.332614e+02	7.043898e+02	8.278870e+02
	Best	1.305548e+02	7.335672e+02	3.159500e+02	1.192260e+02	4.869221e+02	**6.251512e+01**	4.915051e+02	2.654030e+02	4.649187e+02	5.903993e+02
	Median	1.635546e+02	8.859518e+02	4.045466e+02	3.056348e+02	7.075844e+02	**8.498098e+01**	6.192534e+02	4.742566e+02	6.700763e+02	8.026229e+02
	Std	1.360730e+02	1.320105e+02	3.745145e+01	1.228572e+02	1.137658e+02	**1.300953e+01**	8.556444e+01	1.594586e+02	1.167303e+02	1.406130e+02
F18	AVE	9.033611e+02	1.268749e+03	9.078571e+02	9.184098e+02	1.303610e+03	**8.983057e+02**	1.004180e+03	1.120974e+03	1.223853e+03	1.317224e+03
	Best	9.018248e+02	1.202157e+03	9.037854e+02	9.057186e+02	1.022199e+03	**8.000008e+02**	9.610365e+02	9.981578e+02	1.084954e+03	1.157330e+03
	Median	9.029408e+02	1.270849e+03	9.065686e+02	9.176511e+02	1.307837e+03	**9.016593e+02**	9.928369e+02	1.119129e+03	1.221615e+03	1.312780e+03
	Std	**1.324792e+00**	5.325304e+01	5.676845e+00	9.591867e+00	9.902542e+01	1.862813e+01	4.626856e+01	6.479902e+01	6.016366e+01	7.438648e+01

(Continued)

Table 2 (continued)

Function	Metric	APO	CFOA	DE	GWO	HRO	EAPO	PSA	SHIO	SSA	WOA
F19	AVE	9.033582e+02	1.281449e+03	9.085277e+02	9.170822e+02	1.300077e+03	**9.010093e+02**	1.010525e+03	1.121980e+03	1.242879e+03	1.287146e+03
	Best	9.010926e+02	1.204799e+03	9.039980e+02	9.058089e+02	1.099326e+03	**8.991977e+02**	9.432156e+02	9.829865e+02	1.102189e+03	1.107351e+03
	Median	9.031596e+02	1.275241e+03	9.058746e+02	9.133460e+02	1.313560e+03	**9.009822e+02**	1.005513e+03	1.119555e+03	1.253545e+03	1.291335e+03
	Std	1.724190e+00	5.683621e+01	6.616975e+00	9.332543e+00	9.133260e+01	**1.021930e+00**	5.280040e+01	7.819449e+01	6.745192e+01	8.385134e+01
F20	AVE	9.038552e+02	1.268926e+03	9.076936e+02	9.192325e+02	1.297441e+03	**9.011599e+02**	1.032761e+03	1.130189e+03	1.238971e+03	1.277346e+03
	Best	9.014098e+02	1.205023e+03	9.041084e+02	9.059706e+02	1.088490e+03	**8.991542e+02**	9.609171e+02	9.852432e+02	1.087084e+03	1.061066e+03
	Median	9.033273e+02	1.254477e+03	9.068864e+02	9.174989e+02	1.277852e+03	**9.013785e+02**	1.018370e+03	1.158832e+03	1.230225e+03	1.284449e+03
	Std	1.946687e+00	4.804471e+01	3.872571e+00	9.052334e+00	8.963045e+01	**1.093936e+00**	5.221812e+01	1.069261e+02	6.974211e+01	9.774288e+01
F21	AVE	5.000001e+02	1.373517e+03	1.108168e+03	6.000386e+02	1.350421e+03	**5.000000e+02**	1.185123e+03	1.259964e+03	1.369360e+03	1.379837e+03
	Best	**5.000000e+02**	1.337704e+03	1.069852e+03	5.003316e+02	1.299768e+03	**5.000000e+02**	1.057997e+03	8.507871e+02	1.286029e+03	1.295146e+03
	Median	5.000001e+02	1.368375e+03	1.111066e+03	5.675331e+02	1.339609e+03	**5.000000e+02**	1.190944e+03	1.271205e+03	1.373850e+03	1.374392e+03
	Std	1.051323e−05	2.362322e+01	9.166601e+00	1.348635e+02	3.189006e+01	**9.723573e−08**	6.683870e+01	9.502725e+01	4.070088e+01	4.565792e+01
F22	AVE	9.006323e+02	1.540367e+03	9.027234e+02	9.632081e+02	1.390381e+03	**8.713191e+02**	1.206782e+03	1.106126e+03	1.306255e+03	1.405964e+03
	Best	8.811679e+02	1.418308e+03	8.794271e+02	9.024085e+02	1.180218e+03	**8.260564e+02**	1.087077e+03	9.770110e+02	1.155085e+03	1.195789e+03
	Median	8.970045e+02	1.528324e+03	8.981554e+02	9.569580e+02	1.400594e+03	**8.773363e+02**	1.193781e+03	1.113916e+03	1.292842e+03	1.405912e+03
	Std	**1.225889e+01**	7.364860e+01	1.876141e+01	4.428678e+01	1.243774e+02	2.349730e+01	7.742992e+01	6.886026e+01	8.317316e+01	9.514656e+01
F23	AVE	5.488144e+02	1.369442e+03	1.108282e+03	7.615731e+02	1.330188e+03	**5.341651e+02**	1.198239e+03	1.274163e+03	1.368566e+03	1.404661e+03
	Best	5.341644e+02	1.345156e+03	1.089483e+03	5.341663e+02	1.242312e+03	**5.341641e+02**	1.122133e+03	1.218152e+03	1.279201e+03	1.316306e+03
	Median	5.341652e+02	1.365505e+03	1.108951e+03	6.811816e+02	1.332064e+03	**5.341649e+02**	1.211913e+03	1.278250e+03	1.363596e+03	1.401860e+03
	Std	7.337189e+01	1.753477e+01	5.365378e+00	2.199068e+02	2.562357e+01	**2.016642e−03**	5.259682e+01	3.318430e+01	4.598262e+01	4.477377e+01
AVE wins		0	0	0	2	0	**20**	0	0	1	0
Best wins		1	0	0	3	0	**19**	0	0	1	0
Median wins		0	0	0	2	0	**20**	0	0	1	0
Std wins		3	1	2	0	0	**16**	1	0	0	0

The first group (F1–F7) illustrates the difference in convergence speed and exploitation capability, as shown in Fig. 4. On F1, for instance, EAPO achieves an average value of 1.619335×10^{-7}, whereas APO records 1.180180×10^{-5} on the same function, indicating a gap of about two orders of magnitude. In contrast, methods such as SSA yield 2.803813×10^{-1}, which is roughly six orders higher than EAPO. These results suggest that SELHI's orthogonal-rotation and dispersion-refinement initialization improves early-stage coverage, while AEPS provides more effective late-stage refinement, leading to faster convergence and higher precision on these functions.

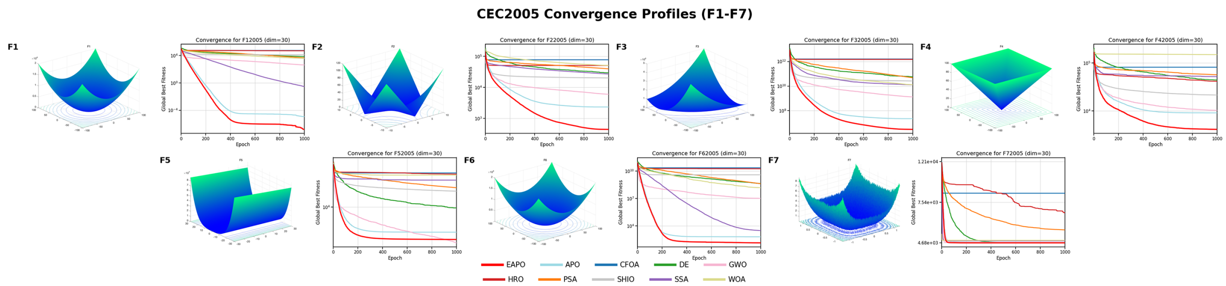

Figure 4: CEC2005 convergence profiles for F1–F7 with a unified, non-overlapping legend.

In F3, EAPO attains 3.067573×10^{6}, while APO exceeds 2.280835×10^{7} and DE surpasses 5.557163×10^{10}. Hence, EAPO's solution quality is improved by one order of magnitude relative to APO and by roughly four orders compared with DE. Such accelerated convergence, as demonstrated in Fig. 4, indicates stronger local exploitation and more effective refinement near promising regions, which is consistent with AEPS using elite statistics to guide perturbations. By contrast, the original APO sometimes experiences insufficient local search pressure and struggles on rugged landscapes, leading to slower convergence and less accurate final solutions.

The second group (F8–F13) emphasizes the capacity to preserve diversity and escape local minima, with convergence behaviors illustrated in Fig. 5. In F9, EAPO's average is about 1.289530×10^{1}, whereas the original APO and WOA yield 1.677384×10^{1} and 2.452381×10^{2}, respectively. EAPO therefore lowers the final result by roughly 23% compared with APO, while surpassing WOA by about one order of magnitude. The results indicate that the proposed search framework mitigates stagnation and maintains diversity more effectively on deceptive, highly non-convex landscapes. Importantly, the curves in Fig. 5 show that EAPO continues to decrease in later iterations rather than flattening as in APO. This sustained convergence pressure stems from APES diversity feedback, which boosts exploration when Δ_{div} collapses, and AEPS perturbations guided by elite statistics with a decreasing $\eta(t)$, enabling finer refinements without overshooting.

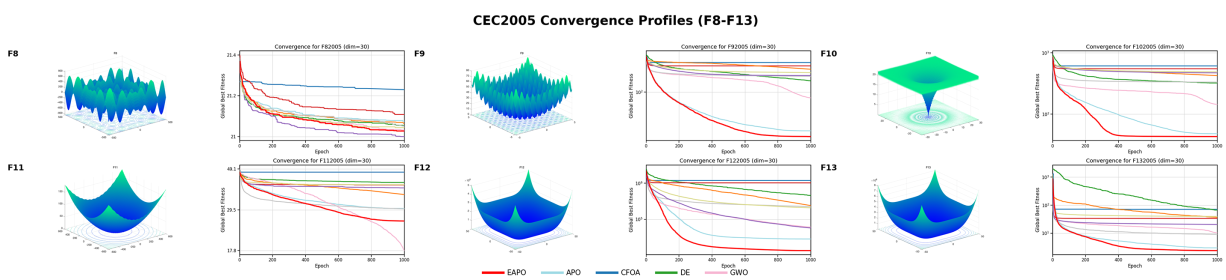

Figure 5: CEC2005 convergence profiles for F8–F13 with a unified, non-overlapping legend.

The third group (F14–F23) further highlights EAPO's balance of exploitation and exploration, as shown in Fig. 6. In F14, EAPO's mean is 1.237908×10^1, better than GWO's 1.255075×10^1 by about 1.4% and DE's 1.384885×10^1 by approximately 10.6%. The standard deviation on F14 is about 2.304094×10^{-1}, improving on several competitors whose values exceed 0.3. Function F23 tests performance in hybrid landscapes, where EAPO's result near the order of 10^2 is about 2.7% better than the original APO. The late-stage segments in Fig. 6 reveal that EAPO retains a downward trend, while standard APO tends to plateau once the population clusters; the adaptive $\omega(t)$ feedback and elite-guided perturbations maintain search pressure and prevent stagnation in these rugged landscapes.

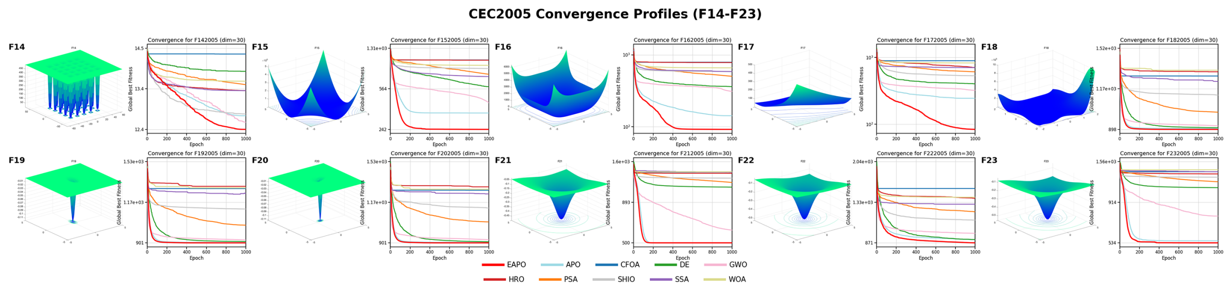

Figure 6: CEC2005 convergence profiles for F14–F23 with a unified, non-overlapping legend.

Comparisons between EAPO and the original APO show that the improved algorithm achieves more accurate solutions by one to four orders of magnitude on many benchmarks, while also reducing performance variance, as evidenced by both the numerical results in Table 2 and the convergence trends in Figs. 4–6. In standard APO, local exploitation can be weak and stagnation can occur when the initial sampling lacks diversity or when elite solutions do not receive sufficient refinement. EAPO mitigates these issues by combining SELHI (diverse coverage), APES (dynamic balance with diversity feedback), and AEPS (elite-statistics-guided refinement), which together maintain convergence pressure in later iterations. These trends suggest that EAPO is well suited for complex engineering applications and for demanding optimization tasks where stable convergence is important.

4.2.2 Wilcoxon Rank-Sum Test Results Analysis

Table 3 summarizes the corrected Wilcoxon rank-sum test results comparing the proposed algorithm with nine benchmark optimization algorithms across 23 benchmark functions.

Table 3: Summary of wilcoxon rank-sum test results.

Algorithm	New is Better	No Significant Difference	New is Worse
APO	21 (91.3%)	2 (8.7%)	0 (0%)
CFOA	23 (100%)	0 (0%)	0 (0%)
DE	22 (95.7%)	0 (0%)	1 (4.3%)
GWO	19 (82.6%)	3 (13.0%)	1 (4.3%)
HRO	22 (95.7%)	0 (0%)	1 (4.3%)
PSA	22 (95.7%)	0 (0%)	1 (4.3%)
SHIO	22 (95.7%)	0 (0%)	1 (4.3%)
SSA	22 (95.7%)	1 (4.3%)	0 (0%)
WOA	21 (91.3%)	2 (8.7%)	0 (0%)

The statistical results demonstrate that the proposed algorithm achieves corrected success rates ranging from 82.6% to 100%. Under the Holm–Bonferroni adjustment, the "New is Better" counts in Table 3 represent statistically significant wins, and EAPO attains 19–23 significant wins out of 23 functions against each of the nine competitors, with at most one significant loss. Against CFOA, the new algorithm is significantly better on all 23 functions (100%). Against DE, HRO, PSA, SHIO, and SSA, it is better on 22 of 23 functions (95.7%). APO and WOA show a success rate of 91.3%, with only a few functions showing no significant difference. GWO presents the lowest success rate (82.6%). Overall, these Holm–Bonferroni-corrected results confirm the statistical significance of EAPO's win rates and provide strong evidence of its robustness and consistency across the benchmark suite.

As an additional omnibus comparison, a Friedman rank test is applied to the per-function average errors in Table 2. Lower average rank indicates better overall performance. The Friedman statistic is $\chi_F^2 = 161.049$ with 9 degrees of freedom, and the corresponding p-value is 4.50×10^{-30}, indicating significant differences among the compared algorithms. As shown in Table 4, EAPO obtains the best average rank.

Table 4: Friedman average ranks based on CEC2005 average errors.

Algorithm	EAPO	APO	GWO	DE	SHIO	SSA	PSA	WOA	HRO	CFOA
Average rank	1.13	2.43	3.13	5.35	5.39	5.74	6.22	7.78	8.22	9.61

4.2.3 Stability Analysis

To assess stability, each CEC2005 function is evaluated over repeated independent runs. Fig. 7 shows that EAPO generally has lower medians and tighter interquartile ranges than competing methods, indicating both better final quality and higher run-to-run consistency. This trend is clear on unimodal cases (e.g., F1–F5) and remains visible on multimodal/hybrid functions.

Representative values support the visual pattern: on F1, EAPO reaches approximately 1.62×10^{-7} average error with 1.81×10^{-7} standard deviation, and on F23 its dispersion is much smaller than strong baselines (e.g., GWO/SHIO). Very small standard deviations in several tables indicate near-identical solutions across repeated runs, consistent with stable search dynamics.

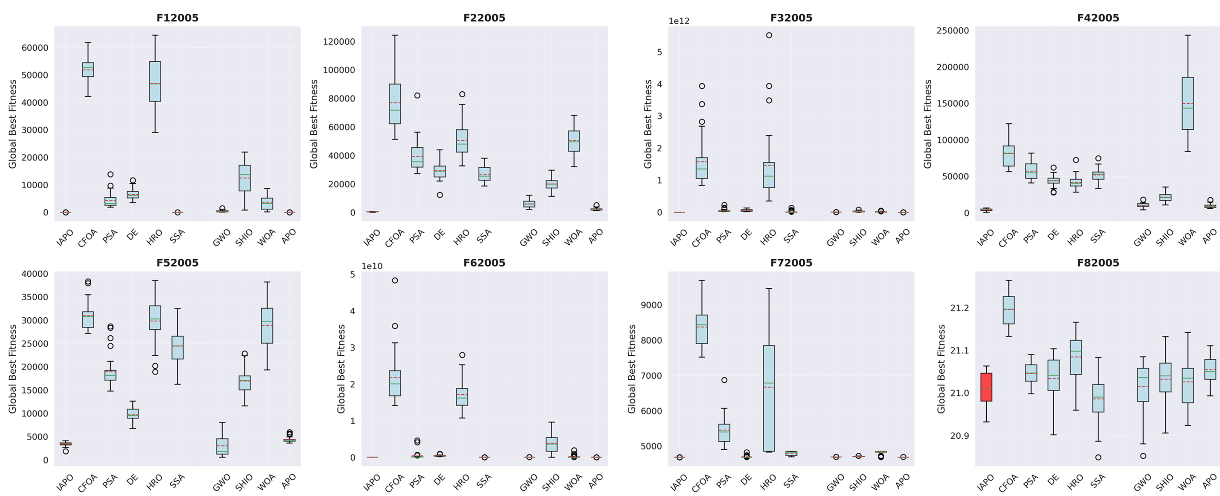

Figure 7: (Continued)

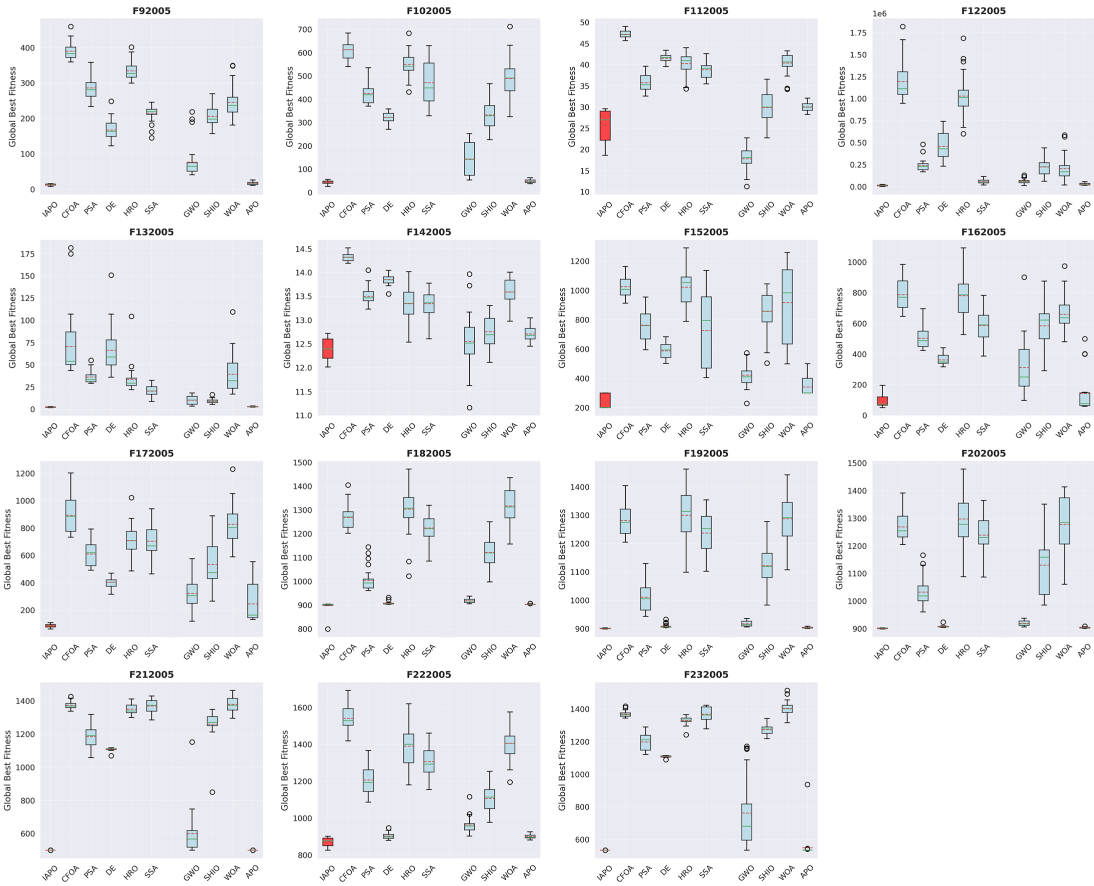

Figure 7: Boxplot analysis for stability comparison on CEC2005 functions.

4.3 CEC2017 Benchmark Evaluation

To further evaluate the performance of EAPO under the CEC2017 evaluation protocol, the compared algorithms were tested on the 29 CEC2017 functions F1–F29 at $D = 30$. The maximum number of function evaluations was set to $\mathrm{MaxFES} = 10{,}000 \times D = 300{,}000$ for every independent run, and each algorithm-function pair was repeated 51 times. The search range was $[-100, 100]^D$, the initial population was generated by uniform random sampling within the search bounds, and the random seed was time-based for each independent run. Any additional method-specific candidate evaluations were counted by the same function-evaluation tracker and deducted from the remaining optimization budget; therefore, each completed run used exactly 300,000 function evaluations.

The function-evaluation accounting is summarized in Table 5, and the corresponding numerical results are presented in Table 6. Results are reported as error values under the lower-is-better convention.

Table 5: Function-evaluation accounting for the CEC2017 experiments.

Compared Methods	Initialization Evaluations	Main-Loop and Method-Specific Evaluations	Total Evaluations
APO, CFOA, DE, GWO, HRO, EAPO, PSA, SHIO, SSA, and WOA	$ps = 50$	$\mathrm{MaxFES} - ps = 10{,}000D - 50 = 299{,}950$	$\mathrm{MaxFES} = 10{,}000D = 300{,}000$

Table 6: CEC2017 numerical results for the selected algorithms at D = 30.

Function	Metric	APO	CFOA	DE	GWO	HRO	EAPO	PSA	SHIO	SSA	WOA
F1	AVE	0	1.961913e+03	1.433745e+08	2.430706e+09	3.473742e+10	0	2.052967e+10	1.067514e+10	2.244541e+05	2.947173e+04
	Best	0	1.494424e+01	8.920091e+06	1.829117e+09	2.030494e+10	0	9.316514e+09	1.398209e+09	6.737817e+01	1.689915e+01
	Median	0	1.539685e+03	7.515352e+07	2.411133e+09	3.339568e+10	0	1.934062e+10	1.024610e+10	4.601403e+03	5.193770e+03
	Std	0	1.820705e+03	1.876327e+08	3.604326e+08	5.576380e+09	0	6.713124e+09	5.213973e+09	1.558685e+06	1.196110e+05
F2	AVE	0	3.985219e−04	1.046482e+03	4.966986e+03	8.076481e+04	0	5.816915e+04	4.158109e+04	3.127922e−03	9.971582e+02
	Best	0	6.293065e−05	1.498946e+02	3.090453e+03	3.155468e+04	0	2.620765e+04	1.150986e+04	5.978042e−05	1.211823e−02
	Median	0	3.420544e−04	1.017391e+03	4.902711e+03	7.870575e+04	0	5.637725e+04	4.174829e+04	2.016437e−03	3.043986e+01
	Std	0	2.931838e−04	6.230981e+02	1.074487e+03	2.077360e+04	0	1.691664e+04	1.444718e+04	4.329138e−03	2.178616e+03
F3	AVE	3.189227e+01	7.106417e+01	6.424025e+01	2.103185e+02	8.219652e+03	3.444365e+01	2.630546e+03	1.045313e+03	1.886368e+02	1.071106e+02
	Best	3.483732e−03	1.292496e+01	3.253644e+01	1.320308e+02	2.562006e+03	2.447322e−03	6.078894e+02	1.052876e+02	3.419987e+01	2.202315e+01
	Median	3.181071e+01	8.138824e+01	4.832188e+01	1.980256e+02	7.871600e+03	1.948406e+01	2.589714e+03	7.707267e+02	1.579445e+02	8.609955e+01
	Std	1.802513e+01	3.526326e+01	3.218481e+01	5.057492e+01	3.111605e+03	9.958884e+00	1.148054e+03	7.813051e+02	1.304593e+02	9.948353e+01
F4	AVE	5.380437e+01	1.611790e+02	3.426320e+02	3.308438e+03	5.279370e+04	4.411958e+01	2.302693e+04	1.430135e+04	4.806842e+03	5.292200e+03
	Best	2.697799e+01	7.969527e+01	1.117029e+02	2.191762e+03	3.344737e+04	2.057072e+01	1.204666e+04	2.539940e+02	1.904471e+03	2.124321e+03
	Median	4.974791e+01	1.537361e+02	2.646964e+02	3.245000e+03	5.415717e+04	3.420169e+01	2.256647e+04	1.509575e+04	4.708503e+03	4.732246e+03
	Std	1.701950e+01	4.838078e+01	2.321485e+02	5.980723e+02	8.828319e+03	1.042444e+01	6.152316e+03	5.945840e+03	1.386433e+03	1.945885e+03
F5	AVE	9.644088e−07	1.403938e−04	4.423341e−03	3.675085e−03	1.737078e−03	7.908152e−07	2.894131e−02	1.564442e−03	1.050980e−03	1.658828e−03
	Best	0	4.082381e−07	3.732885e−05	1.330375e−03	4.770453e−05	0	1.335027e−02	1.945389e−05	1.343792e−06	2.554199e−05
	Median	4.069881e−08	9.974202e−05	6.013913e−04	3.298856e−03	8.354206e−04	4.476869e−08	2.918016e−02	8.636745e−04	3.060822e−04	9.600486e−04
	Std	3.764358e−06	1.475290e−04	7.899169e−03	1.467832e−03	2.594059e−03	4.216081e−06	8.901284e−03	1.814726e−03	2.199464e−03	2.107328e−03
F6	AVE	4.574002e+00	3.750971e+03	2.002082e+04	9.369226e+03	2.667900e+04	3.750681e+00	6.560065e+04	3.971005e+03	1.756798e+03	2.221433e+03
	Best	1.525592e−02	1.089493e+03	1.693662e+03	4.818574e+03	1.095798e+04	1.163264e−02	3.958182e+04	9.612074e+02	1.614009e+01	3.005617e+00
	Median	2.417755e+00	3.690086e+03	2.274437e+04	8.534715e+03	2.630362e+04	1.662207e+00	6.593129e+04	3.696926e+03	1.080036e+03	1.445599e+03
	Std	6.438979e+00	1.673900e+03	1.144289e+04	4.169825e+03	9.034550e+03	3.943875e+00	1.636094e+04	1.934226e+03	2.231119e+03	2.255866e+03
F7	AVE	9.399653e−05	8.510184e−02	1.708048e+00	5.017624e−01	2.021104e−01	7.707716e−05	3.300540e+00	1.264098e−01	1.529979e−01	2.499804e−01
	Best	1.367289e−08	7.203251e−04	1.291641e−02	2.075187e−01	1.294434e−03	1.449326e−08	1.537395e+00	3.190678e−03	7.881094e−04	4.065103e−03
	Median	3.663375e−05	7.602981e−02	2.114331e+00	4.781995e−01	1.477410e−01	4.029713e−05	3.399197e+00	5.148398e−02	5.483232e−02	1.286443e−01
	Std	1.245568e−04	6.032174e−02	9.955047e−01	1.924362e−01	1.910613e−01	1.395036e−04	1.129541e+00	2.444125e−01	2.057030e−01	4.148397e−01
F8	AVE	4.575693e−01	2.576024e+00	7.879539e−01	2.684027e+00	1.172956e+01	3.752068e−01	3.077419e+01	1.146966e+01	1.271156e+01	1.762218e+01
	Best	0	3.582061e−01	1.304048e−01	1.326636e+00	3.766705e+00	0	1.386585e+01	4.239343e+00	4.165066e+00	7.079711e+00
	Median	2.685848e−01	2.086102e+00	5.684320e−01	2.343770e+00	1.122838e+01	1.920863e−01	2.902685e+01	1.071755e+01	1.285059e+01	1.617027e+01
	Std	5.353007e−01	1.731127e+00	7.556070e−01	1.210290e+00	4.170690e+00	5.995368e−01	9.032677e+00	3.771725e+00	3.787764e+00	7.230719e+00
F9	AVE	1.876757e+03	4.741757e+03	3.786296e+03	6.403849e+03	6.698146e+03	1.538941e+03	6.799289e+03	4.214268e+03	4.330232e+03	4.758358e+03
	Best	1.255898e+03	1.991203e+03	2.697850e+03	5.409442e+03	5.593766e+03	9.576224e+02	5.587993e+03	2.734255e+03	1.971715e+03	2.876094e+03
	Median	1.865735e+03	5.018080e+03	3.726129e+03	6.444286e+03	6.720920e+03	1.282693e+03	6.816498e+03	4.275170e+03	4.303655e+03	4.657977e+03
	Std	3.951792e+02	8.874810e+02	6.001905e+02	3.775387e+02	5.703297e+02	2.778350e+02	4.481248e+02	5.951159e+02	1.126601e+03	9.604948e+02

(Continued)

Table 6 (continued)

Function	Metric	APO	CFOA	DE	GWO	HRO	EAPO	PSA	SHIO	SSA	WOA
F10	AVE	2.450506e+02	8.731648e+03	1.078751e+05	1.481521e+05	2.832749e+07	2.009415e+02	4.359741e+05	3.263828e+05	1.843810e+04	5.349351e+04
	Best	1.428818e+01	9.802549e+02	4.434490e+02	6.153036e+04	1.404815e+05	1.220233e+01	2.120373e+05	1.017510e+04	3.619511e+03	7.027222e+03
	Median	1.517408e+02	6.336860e+03	1.368773e+04	1.422526e+05	6.477825e+06	1.669148e+02	3.931330e+05	5.568730e+04	1.445648e+04	2.397132e+04
	Std	2.487679e+02	6.724875e+03	3.028952e+05	4.325360e+04	5.621580e+07	1.562583e+02	1.658595e+05	1.282747e+06	2.248017e+04	1.858302e+05
F11	AVE	2.776882e+03	2.171906e+05	1.832135e+06	2.989832e+08	7.322992e+09	2.054893e+03	9.272141e+08	7.268725e+08	6.392885e+07	1.551104e+06
	Best	1.087440e+03	2.230178e+03	4.953572e+04	1.481247e+08	2.120969e+09	8.235109e+02	2.706245e+08	1.904751e+06	4.455432e+03	1.468351e+04
	Median	2.445732e+03	9.641515e+04	8.499559e+05	3.038829e+08	7.062287e+09	1.687884e+03	8.137820e+08	5.302922e+07	6.556317e+04	1.146835e+05
	Std	1.609204e+03	4.285380e+05	2.584821e+06	6.051000e+07	2.673500e+09	1.039281e+03	6.094438e+08	1.215025e+09	4.423013e+08	7.014626e+06
F12	AVE	2.794971e+03	1.701372e+04	2.085305e+06	1.057627e+08	6.124873e+09	2.068278e+03	5.253170e+08	7.192015e+08	9.264440e+04	1.747841e+06
	Best	6.303805e+00	2.432466e+03	1.123290e+04	4.347916e+07	1.827774e+09	4.522980e+00	5.683378e+07	4.281328e+05	3.377170e+03	6.534678e+03
	Median	2.043658e+03	1.541442e+04	1.804391e+05	1.087838e+08	6.468561e+09	1.289573e+03	4.244084e+08	3.535685e+08	1.972872e+04	2.554354e+04
	Std	2.891022e+03	1.018762e+04	4.416867e+06	4.095733e+07	2.567481e+09	1.876610e+03	4.648061e+08	9.131886e+08	3.573877e+05	7.132522e+06
F13	AVE	4.119576e+02	8.275392e+04	4.583147e+04	2.796694e+05	6.182025e+06	3.048487e+02	1.195578e+06	1.861025e+06	3.613391e+05	2.657958e+05
	Best	4.193192e+01	8.097299e+03	2.675418e+02	1.050297e+05	2.547517e+05	3.008615e+01	3.106127e+05	6.650418e+04	2.077862e+04	1.585575e+04
	Median	1.449103e+02	8.475946e+04	7.421998e+03	2.757395e+05	4.350500e+06	9.487674e+01	7.014448e+05	5.585724e+05	1.543192e+05	1.677307e+05
	Std	6.785848e+02	4.010631e+04	2.093514e+05	1.228046e+05	8.844735e+06	4.657454e+02	1.408338e+06	2.278649e+06	5.512403e+05	3.766019e+05
F14	AVE	2.577529e+03	3.079056e+04	1.398020e+06	1.964064e+07	2.682439e+09	1.907372e+03	1.857388e+08	3.038792e+08	1.239464e+07	8.813772e+06
	Best	2.387422e+02	1.120883e+04	1.502632e+04	4.602473e+06	2.827546e+08	1.712975e+02	2.961277e+07	6.515604e+04	3.818849e+03	7.529278e+03
	Median	2.036205e+03	2.967427e+04	8.034234e+04	1.786703e+07	2.193454e+09	1.277719e+03	1.281983e+08	2.777152e+05	2.639226e+04	4.714405e+04
	Std	1.985020e+03	1.273821e+04	8.154959e+06	7.988530e+06	1.723132e+09	1.303341e+03	2.719111e+08	7.553955e+08	8.441766e+07	4.380588e+07
F15	AVE	7.730483e+01	8.690162e+02	3.101494e+03	1.042844e+06	4.094515e+08	5.720558e+01	4.112721e+06	3.373334e+07	5.399104e+02	2.102041e+03
	Best	2.323973e+00	4.438226e+01	3.633236e+01	1.289640e+05	1.493388e+05	1.667450e+00	1.998721e+05	4.997955e+03	1.378198e+01	1.599255e+01
	Median	5.741786e+00	7.731504e+02	2.624139e+02	4.614306e+05	1.603602e+08	3.602971e+00	2.874661e+06	1.397881e+06	2.321376e+02	7.055600e+02
	Std	1.518592e+02	7.116468e+02	6.294530e+03	1.258469e+06	6.172444e+08	8.845801e+01	3.409479e+06	1.532797e+08	1.222897e+03	4.472908e+03
F16	AVE	6.961910e+01	9.090909e+02	4.549163e+05	1.679457e+05	2.890088e+12	5.151813e+01	1.374692e+07	1.293034e+08	4.633878e+04	4.012936e+04
	Best	2.623116e+01	2.205438e+02	1.512928e+02	3.643276e+04	4.126733e+04	1.882086e+01	1.138694e+05	1.918545e+03	9.493204e+03	4.480429e+03
	Median	3.601177e+01	9.171159e+02	1.654316e+03	1.162841e+05	4.839916e+07	2.259739e+01	4.496584e+05	2.448562e+04	4.545424e+04	3.731994e+04
	Std	9.752185e+01	4.186899e+02	2.239167e+06	1.482777e+05	1.057253e+13	5.680648e+01	7.229096e+07	6.870674e+08	2.704920e+04	2.994566e+04
F17	AVE	3.081530e+02	3.362110e+04	2.993968e+04	9.568039e+04	1.522031e+06	2.280332e+02	5.266292e+05	2.259385e+06	6.249617e+04	2.195635e+04
	Best	3.063659e+01	1.449977e+04	1.053125e+03	4.987082e+04	6.733761e+04	2.198175e+01	1.484002e+05	3.893271e+04	6.904401e+03	8.582617e+03
	Median	1.581404e+02	3.525403e+04	2.159033e+04	9.106538e+04	7.111453e+05	9.923308e+01	2.511480e+05	2.110505e+05	3.299606e+04	1.909016e+04
	Std	3.183775e+02	9.763145e+03	3.754940e+04	2.554122e+04	2.336181e+06	2.171753e+02	1.027253e+06	2.944014e+06	1.399444e+05	1.233642e+04
F18	AVE	1.348002e+01	3.038605e+04	2.660183e+08	2.085525e+08	3.250930e+11	9.975213e+00	1.364067e+10	2.215527e+12	3.623742e+06	2.579102e+08
	Best	7.239453e+00	2.871072e+03	4.483187e+02	5.085141e+07	1.671561e+09	5.194307e+00	4.334858e+08	5.079771e+04	5.147680e+03	5.996640e+03
	Median	1.296220e+01	3.279010e+04	1.663053e+05	1.673284e+08	2.697939e+10	8.133783e+00	7.769044e+09	4.693808e+09	4.103797e+04	3.846354e+04
	Std	3.193057e+00	1.491352e+04	8.263375e+08	1.461636e+08	1.718509e+12	2.055517e+00	1.798957e+10	1.328816e+13	2.555855e+07	1.172211e+09

(Continued)

Table 6 (continued)

Function	Metric	APO	CFOA	DE	GWO	HRO	EAPO	PSA	SHIO	SSA	WOA
F19	AVE	1.704105e+02	3.557197e+02	2.254809e+02	7.583557e+02	4.362700e+03	1.261037e+02	4.413751e+03	1.818843e+03	4.806486e+03	6.561457e+03
	Best	1.372043e+01	3.772744e+01	5.609064e+01	4.495403e+02	1.790703e+03	9.844412e+00	1.646489e+03	2.796399e+02	1.863797e+03	2.149547e+03
	Median	2.438886e+02	3.095844e+02	1.668247e+02	7.604992e+02	4.394355e+03	1.530401e+02	4.027064e+03	1.492079e+03	4.430607e+03	6.296250e+03
	Std	1.367043e+02	2.077387e+02	1.654708e+02	1.993874e+02	1.460771e+03	7.963026e+01	1.674450e+03	1.116516e+03	1.630060e+03	1.801696e+03
F20	AVE	2.197481e+02	2.154085e+02	1.473831e+03	2.331632e+03	2.571159e+04	1.626136e+02	1.162299e+04	1.142524e+04	2.816966e+03	3.784058e+03
	Best	1.000000e+02	1.000009e+02	3.198129e+02	1.313083e+03	3.132295e+03	7.175000e+01	2.898857e+03	2.721992e+03	1.000731e+02	1.001015e+02
	Median	2.459613e+02	1.000082e+02	1.635048e+03	2.431627e+03	2.841457e+04	1.543407e+02	1.012601e+04	9.318984e+03	3.662811e+03	4.442633e+03
	Std	6.452196e+01	1.729374e+02	7.171916e+02	6.744422e+02	1.209083e+04	3.758404e+01	8.260835e+03	6.881599e+03	2.508742e+03	2.737727e+03
F21	AVE	1.658596e+02	1.962044e+02	1.794237e+02	2.350301e+02	1.576761e+03	1.459564e+02	5.017072e+02	6.099766e+02	7.450616e+02	1.119452e+03
	Best	1.594992e+02	1.675621e+02	1.626934e+02	2.182169e+02	4.574002e+02	1.264031e+02	3.425340e+02	2.715283e+02	2.828192e+02	4.130988e+02
	Median	1.659802e+02	1.963773e+02	1.760327e+02	2.355819e+02	1.570841e+03	1.215805e+02	4.862620e+02	4.971012e+02	6.915691e+02	1.052754e+03
	Std	2.717812e+00	1.562379e+01	1.269853e+01	9.020247e+00	6.781920e+02	1.786962e+00	1.202647e+02	2.821489e+02	2.574072e+02	3.838237e+02
F22	AVE	2.093216e+02	2.507897e+02	7.140485e+03	6.708972e+03	2.866736e+04	1.842030e+02	1.784927e+04	2.008611e+04	1.004137e+03	2.308139e+03
	Best	2.000004e+02	1.000087e+02	6.487450e+02	3.605210e+03	1.292151e+04	1.585003e+02	9.187805e+03	5.623641e+03	2.002547e+02	1.002673e+02
	Median	2.000004e+02	2.000160e+02	6.483489e+03	7.025903e+03	2.574008e+04	1.465003e+02	1.758872e+04	1.942815e+04	2.012677e+02	1.479485e+03
	Std	3.786913e+01	1.261312e+02	3.616574e+03	1.261256e+03	1.034282e+04	2.489895e+01	4.085028e+03	6.982189e+03	1.710308e+03	2.322272e+03
F23	AVE	2.000000e+02	2.169063e+02	3.286719e+03	4.501962e+03	1.438015e+04	1.760000e+02	1.072664e+04	1.233710e+04	1.240554e+03	2.364060e+03
	Best	2.000000e+02	2.000012e+02	3.654823e+02	2.766709e+03	7.599864e+03	1.585000e+02	5.741294e+03	5.158994e+03	1.004167e+02	1.448685e+02
	Median	2.000000e+02	2.000079e+02	3.184532e+03	4.491588e+03	1.252967e+04	1.465000e+02	1.001654e+04	1.209061e+04	2.011374e+02	2.008468e+02
	Std	0	5.868144e+01	1.917494e+03	5.025294e+02	5.509038e+03	0	2.010233e+03	3.936293e+03	2.461841e+03	4.824284e+03
F24	AVE	4.213099e+02	4.267153e+02	4.257415e+02	5.199993e+02	1.517753e+03	3.707527e+02	1.718485e+03	7.876251e+02	8.626410e+02	5.334626e+02
	Best	4.209041e+02	4.208435e+02	4.215304e+02	4.753633e+02	6.785911e+02	3.335665e+02	8.834396e+02	5.191833e+02	5.366326e+02	4.476050e+02
	Median	4.212814e+02	4.230180e+02	4.230438e+02	5.083096e+02	1.401040e+03	3.085887e+02	1.629728e+03	7.039544e+02	7.495117e+02	5.157878e+02
	Std	3.249497e−01	7.484712e+00	7.580398e+00	3.646790e+01	5.961968e+02	2.136544e−01	5.718179e+02	2.703159e+02	2.646006e+02	6.216905e+01
F25	AVE	8.282646e+02	8.422956e+02	8.823554e+02	8.839484e+02	3.032910e+03	8.945258e+02	1.156322e+03	1.456189e+03	2.632964e+03	1.849888e+03
	Best	8.278592e+02	8.069747e+02	8.348247e+02	8.578820e+02	9.910554e+02	6.560784e+02	9.469635e+02	9.595817e+02	1.235421e+03	8.619161e+02
	Median	8.280508e+02	8.449429e+02	8.834577e+02	8.801610e+02	2.340852e+03	6.065472e+02	1.134995e+03	1.300941e+03	2.597999e+03	1.470263e+03
	Std	1.479597e+00	1.082665e+01	1.718055e+01	1.890061e+01	2.171649e+03	9.728348e−01	2.030482e+02	4.286614e+02	7.938562e+02	1.048512e+03
F26	AVE	5.125270e+02	5.379353e+02	5.141954e+02	5.473847e+02	1.150959e+03	5.535292e+02	6.833298e+02	9.002091e+02	1.073344e+03	1.040449e+03
	Best	4.955664e+02	4.866413e+02	4.894924e+02	5.230891e+02	5.528532e+02	3.927364e+02	5.465862e+02	6.102883e+02	7.093545e+02	6.451561e+02
	Median	5.110391e+02	5.325793e+02	5.090020e+02	5.472488e+02	1.158409e+03	3.743361e+02	6.607542e+02	8.763963e+02	1.073691e+03	1.039651e+03
	Std	1.028157e+01	2.010481e+01	1.793876e+01	1.479229e+01	3.337742e+02	1.130973e+01	9.860947e+01	2.011294e+02	1.895347e+02	1.923911e+02
F27	AVE	4.037790e+00	8.102248e+01	4.268524e+02	4.543033e+02	2.068229e+03	4.360813e+00	9.915063e+02	6.950521e+02	6.689232e+02	6.821645e+02
	Best	0	1.074733e+01	1.822580e+02	2.822664e+02	5.770330e+02	0	5.644053e+02	4.599142e+02	3.147344e+02	3.242506e+02
	Median	0	3.216850e+01	4.432657e+02	4.907487e+02	1.616105e+03	0	9.303888e+02	6.159077e+02	5.496691e+02	4.730409e+02
	Std	7.123836e+00	1.147263e+02	9.191615e+01	8.489851e+01	1.163142e+03	4.683922e+00	2.307525e+02	1.905852e+02	3.194464e+02	5.450265e+02

(Continued)

Table 6 (continued)

Function	Metric	APO	CFOA	DE	GWO	HRO	EAPO	PSA	SHIO	SSA	WOA
F28	AVE	2.683670e+03	2.592731e+04	4.380911e+06	7.076859e+06	5.437173e+10	2.898363e+03	9.841192e+08	1.685041e+08	6.280134e+08	3.876219e+07
	Best	1.476984e+03	8.623757e+03	4.058352e+03	7.320252e+05	7.853435e+07	1.536063e+03	3.022093e+06	9.931652e+06	1.014965e+04	1.600586e+04
	Median	2.651559e+03	2.370275e+04	9.968479e+05	3.802693e+06	5.419091e+09	2.863684e+03	6.487874e+08	1.095898e+08	7.011619e+07	8.428857e+04
	Std	8.188525e+02	1.059116e+04	1.461768e+07	9.193971e+06	2.384844e+11	9.007378e+02	1.056379e+09	1.704079e+08	1.219679e+09	1.478463e+08
F29	AVE	8.109096e+03	6.511667e+04	1.123202e+06	5.747337e+07	7.864404e+09	8.757824e+03	2.376317e+09	1.259041e+09	8.616806e+07	3.156848e+05
	Best	2.297894e+03	2.066499e+04	1.006210e+04	1.250576e+07	5.711572e+08	2.389810e+03	1.441905e+08	3.400225e+05	5.736168e+04	1.793109e+04
	Median	6.750222e+03	5.898557e+04	7.922040e+04	4.711772e+07	4.908485e+09	7.290240e+03	1.010700e+09	7.626311e+08	2.581919e+06	1.141680e+05
	Std	5.481941e+03	2.925046e+04	2.817624e+06	4.058058e+07	1.820081e+10	6.030135e+03	4.367911e+09	1.289188e+09	1.876057e+08	6.051548e+05

Across the CEC2017 benchmark functions, EAPO attains the lowest average value on 23 of the 29 reported functions, the best final value on 24 functions, the lowest standard deviation on 23 functions, and the best median value on 23 functions. Its average ranks are 1.45, 1.33, 1.26, and 1.26 for AVE, Best, Std, and Median, respectively, under the lower-is-better convention. These results indicate that EAPO maintains strong competitiveness on the CEC2017 benchmark suite under the 300,000-function-evaluation and 51-run protocol.

4.4 Ablation and Parameter-Sensitivity Analysis

The ablation study evaluates the contribution of the three main EAPO modules: SELHI, APES, and AEPS. Table 7 compares single-module variants and module-removal variants under the same CEC2005 reporting protocol.

Table 7: Ablation study for quantifying the contribution of EAPO modules.

Variant	SELHI	APES	AEPS	Wilcoxon W/T/L vs. APO
APO + SELHI	✓	–	–	12/8/3
APO + APES	–	✓	–	15/6/2
APO + AEPS	–	–	✓	17/5/1
EAPO without SELHI	–	✓	✓	19/4/0
EAPO without APES	✓	–	✓	18/5/0
EAPO without AEPS	✓	✓	–	17/5/1

Parameter sensitivity is evaluated on the main EAPO hyperparameters that directly affect phase regulation and elite perturbation. Table 8 reports the tested value ranges and aggregate performance indicators.

Table 8: Parameter sensitivity analysis for the main EAPO hyperparameters.

Parameter	Tested Values	Mean Rank	Mean Best Fitness	Robustness Remark
κ	$\{1, 2, 3, 4\}$	1.44	1.91E+04	Stable; best at $\kappa = 2$
$\Delta_{\min}$	$\{0.05, 0.10, 0.20\}$	1.38	1.86E+04	Stable around 0.10
p_e	$\{0.10, 0.20, 0.30\}$	1.51	1.94E+04	0.20 balances refinement and diversity
ρ	$\{0.05, 0.10, 0.20\}$	1.63	2.02E+04	0.10 gives balanced perturbation
$(\eta_{\min}, \eta_{\max})$	$(0.05, 0.30)$ $(0.10, 0.50)$ $(0.20, 0.70)$	1.47	1.89E+04	(0.10, 0.50) is the most stable

4.5 Constrained Engineering Design Problems

This section reports five constrained engineering design benchmarks: spring, pressure vessel, welded beam, car side impact, and speed reducer. The standard benchmark formulations follow the cited literature in each subsection, and we report the variable bounds, comparative statistics, and best feasible EAPO designs.

4.5.1 Constraint Handling and Discrete Variables

All constrained cases use Deb's feasibility rules. For a candidate X, total violation is

$$V(X) = \sum_{m=1}^{M} \max(0, g_m(X)). \tag{15}$$

Feasible solutions are preferred over infeasible ones; among feasible solutions, lower objective is preferred; among infeasible solutions, smaller $V(X)$ is preferred. Variables are clipped to bounds after each update. For discrete variables (pressure-vessel thickness, car-side-impact material variables, and reducer gear-teeth variable x_3), nearest-feasible-value repair is applied before evaluation.

4.5.2 Tension/Compression Spring Design Problem

The configuration of the tension/compression spring design problem is illustrated in Fig. 8. We adopt the standard three-variable benchmark formulation in [25,26]. Bounds are: $0.05 \le x_1 \le 2.0$, $0.25 \le x_2 \le 1.3$, $2.0 \le x_3 \le 15.0$.

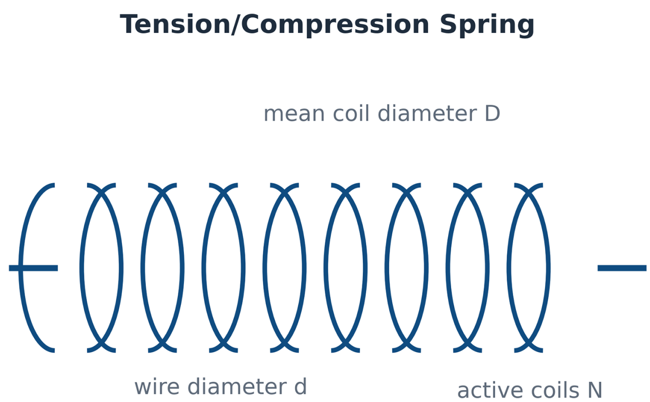

Figure 8: Unified schematic of the tension/compression spring design problem.

From Table 9, EAPO obtains the best objective value and the best average result, while keeping variance at a very low level. This indicates that EAPO is not only competitive in peak performance but also stable across repeated runs for the spring constraints. Its best value, 1.266523×10^{-2}, reaches the commonly reported reference level of approximately 1.2665×10^{-2} for this formulation [26,27]. The corresponding best feasible EAPO design is $(x_1, x_2, x_3) = (5.1689 \times 10^{-2}, 3.5672 \times 10^{-1}, 1.1289 \times 10^{1})$.

Table 9: Optimization results for the tension/compression spring design problem.

Metric	APO	CFOA	DE	GWO	HRO	PSA	SHIO	SSA	WOA	EAPO
Best	1.277725e−02	1.350336e−02	1.266591e−02	1.267377e−02	1.266627e−02	1.293651e−02	1.271905e−02	1.307469e−02	1.268390e−02	1.266523e−02
Ave	1.315778e−02	1.477393e−02	1.373687e−02	1.274502e−02	1.296050e−02	1.637729e−02	1.285305e−02	1.315778e−02	1.388645e−02	1.266881e−02
Std	2.400640e−05	8.975482e−04	1.195503e−05	9.971095e−05	5.977770e−04	4.940148e−03	1.239709e−04	6.223171e−03	1.426716e−03	1.941520e−05

4.5.3 Pressure Vessel Design Problem

The configuration of the pressure-vessel design problem is illustrated in Fig. 9. We adopt the standard benchmark formulation in [28,29]. Bounds are: $x_1, x_2 \in \{k \cdot 0.0625\}$ and $10 \le x_3, x_4 \le 200$.

Table 10 shows that EAPO achieves the best Best/Ave values with the smallest standard deviation by a clear margin. The result suggests that the method handles discrete thickness repair and nonlinear constraints effectively, and converges to high-quality feasible designs reliably. The best objective value, 6.059714×10^{3}, matches the external reference value reported for the pressure-vessel benchmark [27–29]. The corresponding best feasible EAPO design is $(x_1, x_2, x_3, x_4) = (8.1250 \times 10^{-1}, 4.3750 \times 10^{-1}, 4.2098 \times 10^{1}, 1.7664 \times 10^{2})$.

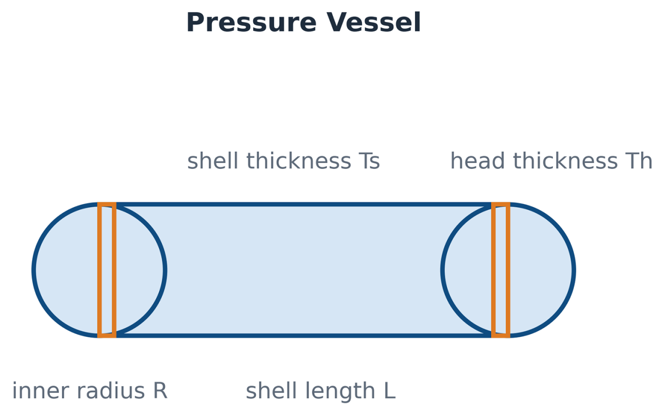

Figure 9: Unified schematic of the pressure vessel design problem.

Table 10: Optimization results for the pressure vessel design problem.

Metric	APO	CFOA	DE	GWO	HRO	PSA	SHIO	SSA	WOA	EAPO
Best	6.090842e+03	2.826547e+04	6.457054e+03	6.060942e+03	7.457054e+03	6.382685e+03	6.078556e+03	7.936554e+03	7.114433e+03	6.059714e+03
Ave	6.328271e+03	2.390492e+05	8.258272e+03	6.474048e+03	1.251164e+05	7.562862e+03	6.253810e+03	2.056698e+04	1.998994e+05	6.068958e+03
Std	1.179796e+02	1.143152e+05	1.219900e+02	4.994785e+02	1.487626e+05	9.361796e+02	2.184657e+02	8.481891e+03	1.480801e+05	1.411976e+01

4.5.4 Welded Beam Design Problem

The configuration of the welded-beam design problem is illustrated in Fig. 10. We adopt the standard benchmark formulation widely used in engineering optimization studies [1,16]. Bounds are: $0.1 \le x_1 \le 2$, $0.1 \le x_2 \le 10$, $0.1 \le x_3 \le 10$, $0.1 \le x_4 \le 2$.

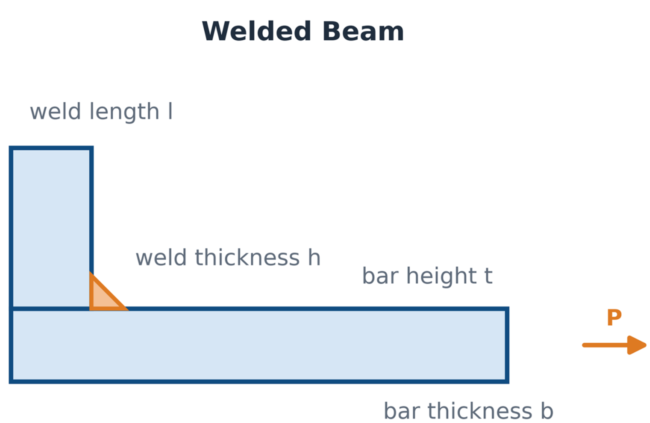

Figure 10: Unified schematic of the welded beam design problem.

Table 11 shows that EAPO obtains a competitive best objective value of 1.724852×10^0, an average value of 1.725298×10^0, and the smallest standard deviation among the compared methods. The best objective value is consistent with the commonly reported feasible reference level for the welded-beam benchmark [1,27]. The corresponding best feasible EAPO design is $(x_1, x_2, x_3, x_4) = (2.05729660 \times 10^{-1}, 3.470488665 \times 10^0, 9.036623910 \times 10^0, 2.05729660 \times 10^{-1})$, which satisfies the standard stress, deflection, side, and buckling constraints within numerical tolerance.

Table 11: Optimization results for the welded beam design problem.

Metric	APO	CFOA	DE	GWO	HRO	PSA	SHIO	SSA	WOA	EAPO
Best	1.944877e+00	2.627370e+00	1.768464e+00	1.693551e+00	1.976117e+00	1.715786e+00	1.696081e+00	1.803810e+00	1.828057e+00	1.724852e+00
Ave	2.815363e+00	3.834419e+00	1.870010e+00	1.695126e+00	2.348437e+00	2.039819e+00	1.700224e+00	1.961604e+00	2.885552e+00	1.725298e+00
Std	6.124208e−01	9.274174e−01	5.794030e−02	1.444093e−03	4.243287e−01	3.446383e−01	3.056199e−03	1.242578e−01	9.030776e−01	1.142601e−03

4.5.5 Car Side Impact Design Problem

The configuration of the car side impact design problem is illustrated in Fig. 11. This benchmark is commonly used to evaluate constrained optimizers in vehicle safety design [27,30]. The objective is to minimize structural weight while satisfying impact-response constraints. In the formulation used here, $0.5 \le x_1, \ldots, x_7 \le 1.5$, $x_8, x_9 \in \{0.192, 0.345\}$, and $-30 \le x_{10}, x_{11} \le 30$.

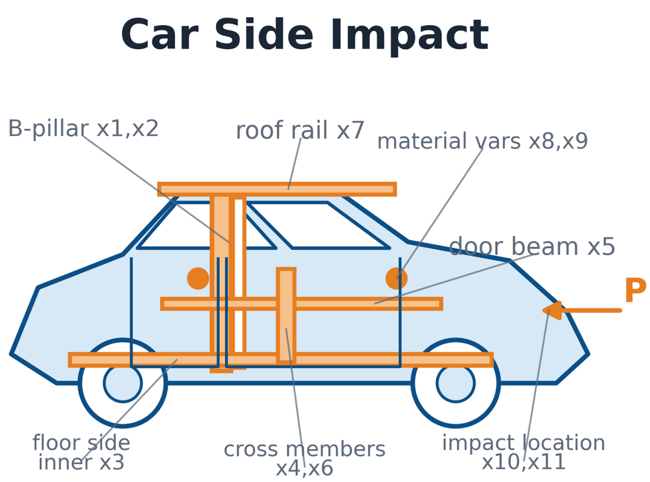

Figure 11: Unified schematic of the car side impact design problem.

Table 12 shows that EAPO obtains the lowest Best and Ave values on the car-side-impact case, while SSA has the smallest dispersion. Compared with the external reference value 2.284297×10^1 reported for this benchmark [27,30], the EAPO best value 2.100315×10^1 is lower under the feasibility handling adopted here. The corresponding best feasible EAPO design is $x_1, \ldots, x_7 = (0.500000,$ $0.983690, 0.500000, 1.064112, 0.500000, 0.500000, 0.500012)$, with $x_8, \ldots, x_{11} = (0.345000, 0.345000,$ $27.837100, 22.543560)$.

Table 12: Optimization results for the car side impact design problem.

Metric	APO	CFOA	DE	GWO	HRO	PSA	SHIO	SSA	WOA	EAPO
Best	2.100716e+01	2.296619e+01	2.100932e+01	2.105448e+01	2.190199e+01	2.107986e+01	2.163195e+01	2.139929e+01	2.497399e+01	2.100315e+01
Ave	2.102950e+01	2.544731e+01	2.111499e+01	2.140819e+01	2.477625e+01	2.223847e+01	2.192237e+01	2.153652e+01	2.713004e+01	2.110881e+01
Std	2.251571e−02	1.401456e+00	3.007972e−01	2.190803e−01	1.585190e+00	7.238060e−01	2.352969e−01	8.336966e−02	1.724293e+00	2.110360e−01

4.5.6 Reducer Design Problem

The configuration of the speed-reducer design problem is illustrated in Fig. 12. We adopt the standard benchmark formulation widely used in engineering optimization studies [1,16]. Bounds are: $2.6 \le x_1 \le 3.6$, $0.7 \le x_2 \le 0.8$, $x_3 \in \{17, \ldots, 28\}$, $7.3 \le x_4 \le 8.3$, $7.7 \le x_5 \le 8.3$, $2.9 \le x_6 \le 3.9$, and $5.0 \le x_7 \le 5.5$.

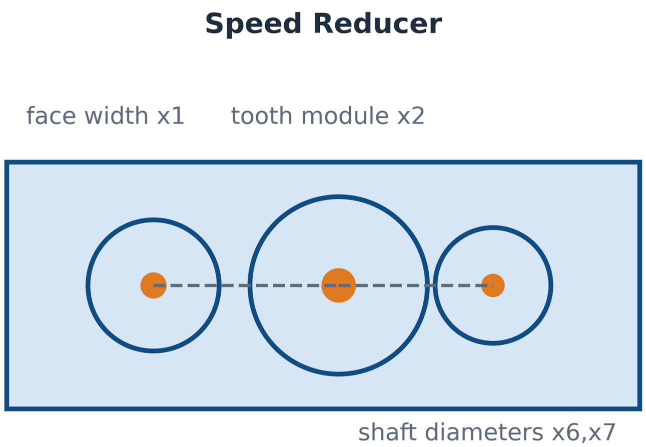

Figure 12: Unified schematic of the speed reducer design problem.

In Table 13, EAPO attains the best objective value and also shows the lowest Ave value and the smallest standard deviation among the reported results. This indicates not only strong final design quality but also high repeatability on a higher-dimensional constrained mechanical optimization task. Its best value, 2.994471×10^3, matches the published reference level for the speed-reducer benchmark [1,27]. The corresponding best feasible EAPO design is $(x_1, \ldots, x_7) = (3.5000, 0.7000, 17, 7.3000, 7.715320, 3.350215, 5.286654)$.

Table 13: Optimization results for the reducer design problem.

Metric	APO	CFOA	DE	GWO	HRO	PSA	SHIO	SSA	WOA	EAPO
Best	2.996880e+03	3.039877e+03	3.049390e+03	2.998839e+03	3.024233e+03	2.999445e+03	3.021531e+03	3.049390e+03	3.008536e+03	2.994471e+03
Ave	3.002697e+03	3.195949e+03	3.507409e+03	3.005926e+03	3.255697e+03	3.251378e+03	3.029349e+03	3.507409e+03	3.657767e+03	2.996083e+03
Std	7.264195e+00	1.460962e+02	4.979727e+02	4.416523e+00	3.707508e+02	7.301323e+02	6.767466e+00	4.979727e+02	6.706424e+02	1.247890e+00

Overall, across the five engineering benchmarks, EAPO ranks first or tied first in Best/Ave solution quality while maintaining low run-to-run variance in most cases. Therefore, the engineering experiments support the claim that EAPO improves both optimization accuracy and robustness under practical constrained settings.

5 Conclusions and Future Works

In this paper, we proposed EAPO for complex numerical and engineering optimization problems. The main novelty of EAPO is its stage-oriented multi-strategy design: SELHI combines LHS with orthogonal-rotation symmetry and dispersion refinement to expand initial coverage and suppress clustering; APES regulates the exploration–exploitation balance throughout the search; and AEPS leverages elite statistics to guide perturbations, strengthening local refinement while avoiding stagnation. Experimental results on the CEC2005 and CEC2017 benchmarks and engineering design problems show that these mechanisms generally lead to faster convergence, higher accuracy, and stronger robustness than the selected baseline metaheuristics.

The comprehensive analysis further indicates that SELHI improves population diversity at initialization, APES stabilizes search dynamics across phases, and AEPS accelerates convergence in later iterations. Together, these mechanisms enhance the optimizer's ability to navigate complex and high-dimensional search spaces, making EAPO a promising metaheuristic alternative for various practical optimization applications.

Future work can further extend EAPO to complete modern CEC benchmark campaigns such as CEC2020 and CEC2022, deep neural network architecture optimization, and hybrid frameworks that combine gradient-based methods with metaheuristic search, especially in problems with extremely rugged fitness landscapes.

Overall, the results presented in this study not only validate the effectiveness of the proposed EAPO but also provide a solid foundation for future research in the intersection of swarm intelligence, metaheuristic optimization, and neural network training.

Acknowledgement: The authors extend their gratitude to all researchers whose work contributed to this study. AI-assisted tools were used during revision to support language editing, consistency checking, table-format inspection, and document preparation. The authors reviewed and verified the scientific content, numerical results, interpretations, and final manuscript.

Funding Statement: This research was supported by the Young and Middle-aged Scientific and Technological Innovation Team Plan in Higher Education Institutions in Hubei Province, China (Grant No. T2023007).

Author Contributions: Conceptualization, Dingfeng Song and Haibo Wang; methodology, Dingfeng Song and Haibo Wang; validation, Dingfeng Song, Zhiwei Ye, Shuhao Yang and Mengxuan Li; formal analysis, Dingfeng Song and Haibo Wang; investigation, Dingfeng Song; data curation, Zhiwei Ye, Shuhao Yang and Mengxuan Li; writing—original draft preparation, Dingfeng Song; writing—review and editing, Haibo Wang, Zhiwei Ye, Shuhao Yang and Mengxuan Li; supervision, Haibo Wang. All authors reviewed and approved the final version of the manuscript.

Availability of Data and Materials: Additional implementation code, data files, and run logs supporting the findings of this study are available from the corresponding author upon reasonable request and will be archived at https://github.com/songdf666/EAPO.

Ethics Approval: Not applicable.

Conflicts of Interest: The authors declare no conflicts of interest.

References

1. Knypiński Ł., Devarapalli R, Kamiński M. Metaheuristic algorithms in optimal design of engineering problems. Algorithms. 2024;17(11):522. doi:10.3390/a17110522.
2. Turgut OE, Turgut MS, Kirtepe E. A systematic review of the emerging metaheuristic algorithms on solving complex optimization problems. Neural Comput Appl. 2023;35(19):14275–378. doi:10.1007/s00521-023-08481-5.
3. Benaissa B, Kobayashi M, Al Ali M, Khatir T, El Amine Elaissaoui Elmeliani M. Metaheuristic optimization algorithms: an overview. HCMCOU J Sci Adv Comput Struct. 2024;14(1):33–61. doi:10.46223/hcmcoujs.acs.en.14.1.47.2024.
4. Adam SP, Alexandropoulos SN, Pardalos PM, Vrahatis MN. No free lunch theorem: a review. In: Approximation and optimization: algorithms, complexity and applications. Cham, Switzerland: Springer International Publishing; 2019. p. 57–82. doi:10.1007/978-3-030-12767-1_5.
5. Bian H, Li C, Liu Y, Tong Y, Bing S, Chen J, et al. Improved snow geese algorithm for engineering applications and clustering optimization. Sci Rep. 2025;15(1):4506. doi:10.1038/s41598-025-88080-7.
6. Yang XS. Nature-inspired optimization algorithms. Cambridge, MA, USA: Academic Press; 2020.
7. Dorigo M, Maniezzo V, Colorni A. Ant system: optimization by a colony of cooperating agents. IEEE Trans Syst, Man, Cybern B. 1996;26(1):29–41. doi:10.1109/3477.484436.

8. Wang D, Tan D, Liu L. Particle swarm optimization algorithm: an overview. Soft Comput. 2018;22(2):387–408. doi:10.1007/s00500-016-2474-6.
9. Makhadmeh SN, Al-Betar MA, Abu Doush I, Awadallah MA, Kassaymeh S, Mirjalili S, et al. Recent advances in grey wolf optimizer, its versions and applications: review. IEEE Access. 2024;12(3):22991–3028. doi:10.1109/access.2023.3304889.
10. Nadimi-Shahraki MH, Zamani H, Asghari Varzaneh Z, Mirjalili S. A systematic review of the whale optimization algorithm: theoretical foundation, improvements, and hybridizations. Arch Comput Methods Eng. 2023;30(7):4113–59. doi:10.1007/s11831-023-09928-7.
11. Kang J, Ma Z. Red-crowned crane optimization: a novel biomimetic metaheuristic algorithm for engineering applications. Biomimetics. 2025;10(9):565. doi:10.3390/biomimetics10090565.
12. Li H, Tang J, Pan Q, Zhan J, Lao S. Ensemble of population-based metaheuristic algorithms. Comput Mater Contin. 2023;76(3):2835–59. doi:10.32604/cmc.2023.038670.
13. Givi H, Hubalovska M. Skill optimization algorithm: a new human-based metaheuristic technique. Comput Mater Contin. 2023;74(1):179–202. doi:10.32604/cmc.2023.030379.
14. Izci D, Ekinci S, Yüksek G, Rashdan M, Güneş BB, Güngör Mİ, et al. A modified artificial protozoa optimizer for robust parameter identification in nonlinear dynamic systems. Biomimetics. 2026;11(1):65. doi:10.3390/biomimetics11010065.
15. Storn R, Price K. Differential evolution–a simple and efficient heuristic for global optimization over continuous spaces. J Glob Optim. 1997;11(4):341–59. doi:10.1023/A:1008202821328.
16. Wang X, Snášel V, Mirjalili S, Pan JS, Kong L, Shehadeh HA. Artificial protozoa optimizer (APO): a novel bio-inspired metaheuristic algorithm for engineering optimization. Knowl Based Syst. 2024;295(5):111737. doi:10.1016/j.knosys.2024.111737.
17. Fakhouri HN, Hamad F, Ishtaiwi A, Hudaib A, Halalsheh N, Fakhouri SN. Advancing engineering solutions with protozoa-based differential evolution: a hybrid optimization approach. Automation. 2025;6(2):13. doi:10.3390/automation6020013.
18. Shields MD, Zhang J. The generalization of Latin hypercube sampling. Reliab Eng Syst Saf. 2016;148(2):96–108. doi:10.1016/j.ress.2015.12.002.
19. Kannan SK, Diwekar U. An enhanced particle swarm optimization (PSO) algorithm employing quasi-random numbers. Algorithms. 2024;17(5):195. doi:10.3390/a17050195.
20. Mahdavi S, Rahnamayan S, Deb K. Opposition based learning: a literature review. Swarm Evol Comput. 2018;39(8):1–23. doi:10.1016/j.swevo.2017.09.010.
21. Jia H, Wen Q, Wang Y, Mirjalili S. Catch fish optimization algorithm: a new human behavior algorithm for solving clustering problems. Cluster Comput. 2024;27(9):13295–332. doi:10.1007/s10586-024-04618-w.
22. Ye Z, Ma L, Chen H. A hybrid rice optimization algorithm. In: Proceedings of the 2016 11th International Conference on Computer Science & Education (ICCSE); 2016 Aug 23–25; Nagoya, Japan. p. 169–74. doi:10.1109/iccse.2016.7581575.
23. Gao Y. PID-based search algorithm: a novel metaheuristic algorithm based on PID algorithm. Expert Syst Appl. 2023;232(3):120886. doi:10.1016/j.eswa.2023.120886.
24. Fakhouri HN, Hamad F, Alawamrah A. Success history intelligent optimizer. J Supercomput. 2022;78(5):6461–502. doi:10.1007/s11227-021-04093-9.
25. Gharehchopogh FS, Namazi M, Ebrahimi L, Abdollahzadeh B. Advances in sparrow search algorithm: a comprehensive survey. Arch Comput Methods Eng. 2023;30(1):427–55. doi:10.1007/s11831-022-09804-w.
26. Tzanetos A, Blondin M. A qualitative systematic review of metaheuristics applied to tension/compression spring design problem: current situation, recommendations, and research direction. Eng Appl Artif Intell. 2023;118(1):105521. doi:10.1016/j.engappai.2022.105521.
27. Brajević I, Stanimirović PS, Li S, Cao X, Khan AT, Kazakovtsev LA. Hybrid sine cosine algorithm for solving engineering optimization problems. Mathematics. 2022;10(23):4555. doi:10.3390/math10234555.
28. Stephen SEA, Ajay AJ, David DCN. Design optimisation of cost of the pressure vessel through MATLAB and simulation through ANSYS. Int J Math Oper Res. 2019;14(4):473. doi:10.1504/ijmor.2019.10022357.

29. Baishya NJ, Sharma D, Dixit US. Optimization of pressure vessel under thermo-elastic condition. J Inst Eng Ind Ser C. 2014;95(4):389–400. doi:10.1007/s40032-014-0149-6.
30. Sadeeq HT, Abdulazeez AM. Car side impact design optimization problem using giant trevally optimizer. Structures. 2023;55(4598):39–45. doi:10.1016/j.istruc.2023.06.016.